Effect Of Wire Electro Discharge Machining Parameters On Surface Roughness Of D2 Tool Steel

Dr. Dhobe Milind M.
PES College of Engineering, Aurangabad (M.S.) India

Abstract: *Wire Electrical Discharge Machining (WEDM) is a nontraditional electro-thermal machining process capable of machining parts having complicated shapes and higher hardness. Materials having higher hardness are difficult to machine by traditional machining process. The technology on which WEDM works is conventional electro discharge sparking phenomenon widely accepted and implemented for industrial applications. In this paper, the effect of various heat treatment processes and machining parameters of WEDM like pulse on time (T_{ON}), pulse off time (T_{OFF}), gap voltage (S_V), peak current (IP) has been investigated to reveal their impact on surface roughness of tool steel AISI D2. During this research work, it is tried to investigate the effect of one variable at a time. The efforts are made to set the process parameters to minimize the surface roughness. The experimental studies were carried on Electronica Spring Cut WEDM machine and surface roughness is measured using Hommel Surface Roughness Tester T8000.*
It is observed that the surface roughness increases with increase in pulse on time (T_{ON}) and peak current (IP) while decreases with increase in number of tempering cycles after hardening for the same process parameters.

Keywords: **Tool steel, Hardening, Tempering, WEDM, Surfaceroughness**

1. Introduction

Due to the advancement in Engineering and technology demand for tool steel materials having higher hardness and impact resistance is increasing. Nevertheless these materials are difficult to machine using traditional methods. Hence, nontraditional machining methods such as Electro Discharge Machining and Wire Electro Discharge Machining (WEDM) are applied. Before designing the dies, proper choice of tool steel is important to insure good performance. Tool steels are selected based on one of the property such as non-deformability, toughness, Wear resistance, machineability and brittleness. Heat treatment is the process by which required properties can be inculcated in order to obtain the desired characteristics in the material. In Wire-EDM process a thin wire as an electrode is used to machine the surface The Wire-machined surface consists of many craters caused by electrical spark. The larger the electrical discharging energy, the worse is the surface quality. A large energy will produce a rippled surface and changes the structural and physical properties of the materials.

Many researchers have carried experiments by varying the machining parameters and analyzing the properties. It is observed that surface roughness is affected by Pulse duration and discharge current in WEDM. By decreasing the pulse duration and discharge current surface roughness can be improved [8]. Further it has been observed that if pulse energy per discharge is kept constant, short pulses and long pulses gives same surface roughness. However the surface topography and material removal rate will be different. The short pulse duration gives higher material removal rate than the long pulse duration [1]

Experimentally it is observed that if the discharge energy is kept constant the short duration pulse and a high peak value discharge current removes the material by

gasifying while a long duration pulse and low peak discharge current removes the material from the work piece by melting [2].

In WEDM, the parameters wire feed and wire tension have no effect on material removal rate. The pulse on time directly affects the material removal rate and surface roughness. Increase in pulse on time and peak current increases the material removal rate and decreases the surface roughness. It is further observed that due to increase in pulse off time and servo voltage decreases the MRR but improves the surface quality [3].

During W-EDM enormous amount of heat generated causes local melting or even evaporation the work piece surface and electrode material. Similarly it causes the vaporization of dielectric fluid, which creates high pressure and forces the molten as well as vaporized material into finer particles in all directions. Continuous flow of dielectric fluid carries the droplets of metal away from the parent metal; however some of the molten metal solidified on work piece contributes to increasing the surface roughness [4].

After multi cut WEDM, the machined surface shows microstructure of fine martensitic behavior in tool steels due to rapid heating and instant cooling by dielectric fluid. After third and fourth cut a thin white layer composed of fine martensite and surface alloying in the work piece adjacent to the third and fourth cut surface was observed. The higher degree of surface alloying between wire electrode and work piece material was observed after fifth cut [7].

2. Experimental Methodology

The machine used for experimentation work was "spring cut" Electronica Make Wire EDM as shown in the Figure 1. The test material used is AISI D2 steel and its composition is as shown in the Table 1.

Figure 1: Wire Electro Discharge Machine

Table 1: AISI D2 Material Composition						
Element / AISI D2	C	Si	Mn	Cr	Mo	V
%	1.57	0.4	0.51	12.5	0.41	0.25

CuZn37 master brass wire with 0.25 mm diameter having tensile strength of 900 N/mm^2 was used as an electrode. De-ionized water (Ph Value 12.5) was used as the dielectric medium. The specimens of tool steel AISI D2 of 10 □ 10 □ 50 mm size were prepared by milling. The specimens are then heat treated in two different ways. The first one is Single Tempering (ST) after hardening and the other is Double Tempering (DT) after hardening. The heat treatment was then followed by W-EDM process to obtain 10 □ 10 □ 4 mm thick test pieces. During machining, the parameters, i.e., pulse interval time (16 µs), table feed rate (7.6 mm/min), Wire tension (1800 g), pulse current on, pulse Current off, and Voltage were kept constant. A surface finish Tester (Taylor Hobson make) was used to measure the surface roughness.

3. Observations

Number of experiments was conducted to find out the effect of input parameters on output parameter. During the experimentation the input parameters considered are pulse on time (T_{ON}), Pulse off (T_{OFF}), Servo voltage (S_v) and Peak current (I_p) one at a time are considered to find out its effect on output parameter. The output parameter is Surface roughness. The change in output parameter due to change in input parameter is measured every time.

3.1 Effect of T_{ON}

In the first set of experiment pulse on time was varied from 105 units to 125 units in step of 5 units. All other parameters such as servo voltage, wire feed, peak current, and wire tension were kept constant. The variation in surface roughness due to variation in pulse on time is tabulated in the Table 2.

Table 2: Effect of T_{ON}			
S. No.	Parameter	Ra µm	
	T_{ON} (Units)	Single Tempered	Double Tempered
1.	105	1.34	1.28
2.	110	2.21	1.51
3.	115	3.34	1.97
4.	120	3.39	2.17
5.	125	3.45	2.59

The other parameters kept constant during first set of experiment are: T_{OFF} = 40, Sv = 15, I_p = 70, W_f = 5, W_t = 9, S_f = 2100, Cc = 5, V_p = 2, W_p = 1, S = 20/12, Wire Dia. = 0.25 mm.

3.2 Effect of T_{OFF}

In the second set of experiment pulse off time (T_{OFF}) was varied from 40 units to 60 units in step of 5 units. All other parameters such as pulse on time, servo voltage, wire feed, peak current, wire tension were kept constant. The variation in surface roughness due to variation in pulse off time tabulated in Table 3 and is shown graphically in the Figure 3. The parameters kept constant during second set of experiment are: T_{ON}=70, W_f = 5, W_t = 9, S_f = 2100, Cc = 5, V_p = 2, W_p = 1, S = 20/12, Wire Dia. = 0.25 mm

Table 3: Effect of T_{OFF}

S. No.	Parameter	Ra µm	
	T_{OFF} (Units)	Single Tempered	Double Tempered
1.	40	2.56	2.47
2.	45	2.43	2.21
3.	50	1.92	1.71
4.	55	1.72	1.65
5.	60	1.34	1.28

3.3 Effect of Sv

In the third set of experiment servo voltage is varied from 15 units to 45 units in step of 5 units. All other parameters such as pulse on, pulse off time, wire feed, peak current, wire tension were kept constant. The variation in surface roughness due to variation in servo voltage is tabulated in the Table 4. The parameters kept constant during third set of experiment are: T_{ON} = 105, T_{OFF} = 40, I_p = 70, W_f = 5, W_t = 9, S_f = 2100, Cc = 5, V_p = 2, W_p =1, S = 20/12, Wire Dia. = 0.25 mm.

Table 4: Effect of Sv

S. No.	Parameter	Ra µm	
	Sv (Units)	Single Tempered	Double Tempered
1.	15	1.342	1.28
2.	20	1.287	1.22
3.	25	1.193	1.10
4.	30	1.180	1.08
5.	35	1.163	1.05
6.	40	1.154	1.04
7.	45	1.055	1.03

3.4 Effect of I_p

In the fourth set of experiment peak current is varied from 70 units to 110 units in step of 10 units. All other parameters such as pulse on, pulse off time, wire feed, peak current, wire tension were kept constant. The variation in surface roughness due to variation in Peak current is tabulated in the Table 5 and is graphically shown in the Figure 5. The parameters kept constant during fourth set of experiment are: T_{ON} = 105, Sv = 15, T_{OFF} = 40, W_f = 5, W_t = 9, S_f = 2100, Cc = 5, V_p = 2, W_p = 1, S = 20/12, Wire Dia. = 0.25 mm

Table 5: Effect of I_p

S. No.	Parameter	Ra µm	
	I_p (Units)	Single Tempered	Double Tempered
1.	70	1.342	1.28
2.	80	1.564	1.78
3.	90	2.209	1.89
4.	100	2.183	1.67
5.	110	2.063	1.54

4. Result And Analysis

While conducting the various experiments during this study one factor experimental strategy was adopted. As per this strategy only one input parameter is to be varied at a time and all other input parameters are to be kept constant. During this experimental work in all twenty two experiments were conducted over two different types of test pieces. The various experimental results observed areanalyzed and presentedhere.

4.1 The effect of pulse on time (T_{ON}) on the surface roughness is shown graphically in Figure 2. The graph shows that the surface roughness obtained in double tempered test piece sample is lower than the values obtained in single tempered test piece samples. In both the cases surface roughness increases with increase in Ton value. The pattern of variation followed is nearly same in both the cases

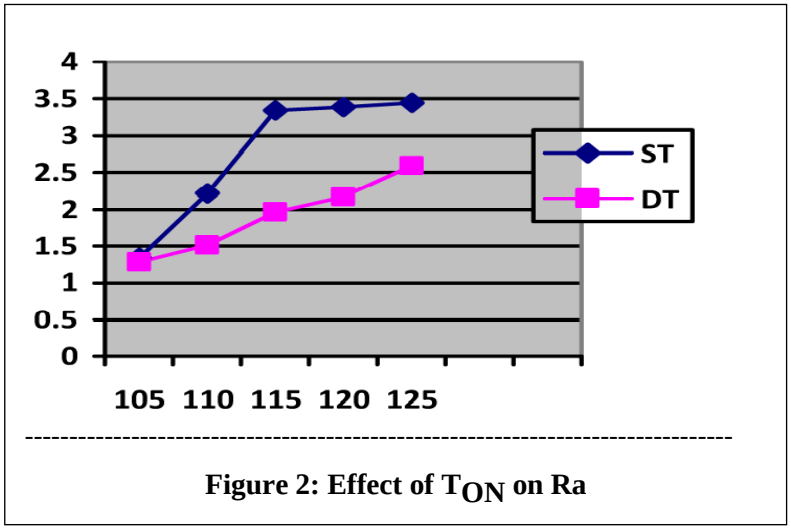

Figure 2: Effect of T_{ON} on Ra

4.2 Effect of T_{OFF} on Ra—for the second set of experiments the effect of pulse off time (T_{OFF}) on surface roughness is graphically shown in the Figure3. The graph shows that in both the cases surface roughness decreases with increase in pulse off time. The roughness values obtained in case of hardened and double tempered test piece are slightly lower or equal to the values obtained in case of single tempered test piecesamples

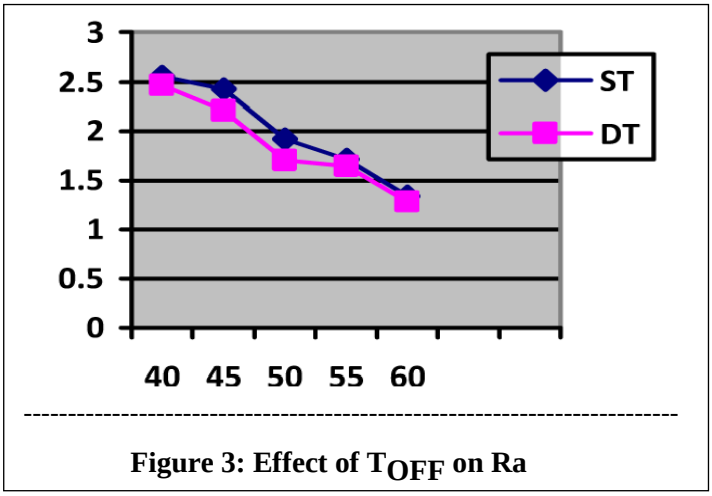

Figure 3: Effect of T_{OFF} on Ra

4.3 Effect of Sv on Ra—for the third set of experiments the effect of Servo voltage Sv on surface roughness is shown in the Figure 4. The graph shows that surface roughness decreases with increase in servo voltage. The roughness values obtained in double tempered test piece sample are lower than that of single tempered test piece

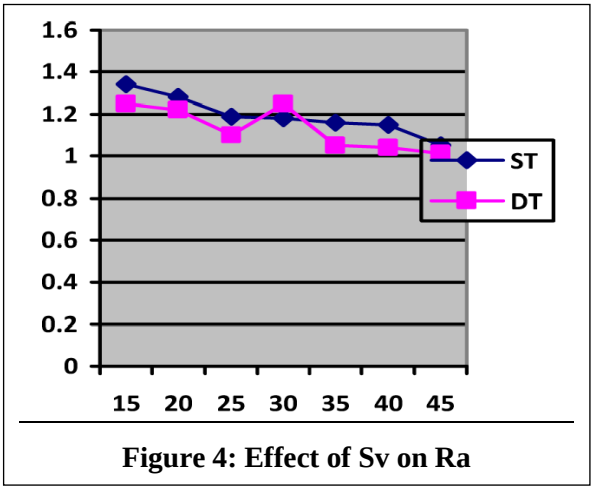

Figure 4: Effect of Sv on Ra

4.4 Effect of peak current Ip—for the next set of experiment the effect of peak current on surface roughness is as shown in the Figure 5. The graph shows that the roughness first slightly increases and then decreases with increase in peak current. However the increase in roughness due to increase in peak current in case of double tempered test piece is less than that of single tempered test piece and the pattern of variation in roughness is near about same in case of both the type of test pieces.

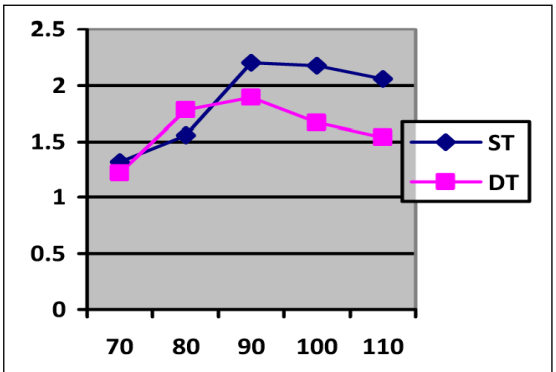

Figure 5: Effect of I_D on Ra

5. Conclusion

On the basis of experimental study conducted and the result obtained the conclusions drawn are as follows:

- With increase in pulse on time surface roughness increases in both the type of test pieces. However for the same increasing values of pulse on time the surface roughness is lower in case of double tempered test piece than that of single tempered test piece samples.
- With the increase in pulse off time there is a continuous decrease in surface roughness in both the types of test pieces. Hardened and double tempered test piece gives lower surface roughness, however the difference in surface roughness values obtained in both the type of test pieces is very less.
- With the increase in servo voltage there is small decrease in surface roughness in case of both the types of test piece samples. It means that the surface quality improves with the increase in servo voltage.
- With the increase in peak current surface roughness increases in both the types of test pieces and afterwards it decreases. The surface roughness in double tempered test piece is lower than that of single tempered test piece.
- As a overall concluding remark we can say that the surface roughness increases with increase in Pulse on time and Peak current, while decreases with increase in pulse off time and servo voltage. Similarly double tempering after hardening reduces surface roughness compared to single tempering.

6. Acknowledgement

Authors express their sincere thanks to the Metallurgy and Material science Department VNIT, Nagpur, Marathwada Institute of Technology, Aurangabad, University Department of Chemical Technology, Dr. B.A.M.U., Aurangabad, Vision Tool Tech. and Avinash Enterprises (Tool Design and Manufacturing), Shree Saigan Industries, and Sidheshwar Wire Cut, MIDC Waluj, Aurangabad for supporting and extending Machining and testing facilities.

7. REFERENCES

1. *Ahmet Hascalyk and Ulas Catdas, "Experimental Study of Wire Electrical Discharge Machining of AISID5 Tool Steel", Journal of Material Processing and Technology, Vol. 148, (2004), p. 362.*
2. *Akhmedpasheav M Y U, "A Study of Heat Treated Carburized Alloyed Steels for Blanking Dies", Journal of Material Science and Heat Treatment, Vol. 49, (2007), p.11.*
3. *Ashan Ali Khan, Munira Bt Mohd Ali and Norhashimah Bt Mohd Shaffiar, "Relationship of Surface Roughness with Current and Voltage During W-EDM", Journal of Applied Science, Vol. 6, No. 10, (2006), p.2317.*
4. *Bosheh S S and Mativenga P T , "White Layer Formation in Hard Turning of H13 Tool Steel at High Cutting Speed Using CBN Tooling", International Journal of Machine Tools and Manufacture, Vol. 46, (2006), p.225.*
5. *Che-Chung Wang, Han-Ming Chow, Lieh- Dai Yang and Chun-Te Lu "Recast Layer Removal After Electrical Discharge Machining via Taguchi Analysis: A Feasibility Study", Journal of Material Processing and Technology, (2009), p. 4134.*
6. *Choi K K, Nam W J and Lee Y S "Effects of Heat Treatment on the Surface of a Die Steel STD 11 Machined by W- EDM", Journal of Material Processing and Technology, Vol. 201, (2008), p.580.*
7. *Huang CA, Hsu C C and Kuo H H "The Surface Characteristics of P/M High- Speed Steel (ASP 23) Multi-Cut with Wire Electrical Discharge Machine (WEDM)", Journal of Material Processing and Technology, Vol. 140, (2003), p.298.*
8. *Rebelo J C, Moarao A, Kremer D and Lebrun J L, "Influence of EDM Pulse Energy on the Surface Integrity of Martensitic Steels", Journal of Material Processing and Technology, Vol. 84, (1998) p. 90.*
9. *Sing H and Garg R, "Effect of Process Parameters on Material Removal Rate in WEDM", Journal of Achievements in Materials and Manufacturing Engineering, Vol. 32, (2009), pp. 70-74.*

International Journal of Advances in Scientific Research and Engineering (ijasre)

E-ISSN : 2454-8006

DOI: 10.31695/IJASRE.2023.9.3.2

Volume 9, Issue 3
March - 2023

Modelling and Simulation of Acceleration Model of Small Electric Motor Vehicle

Ramesh G Pungle

Associate Professor

Department of Mechanical and Automation Engineering

P. E. S. College of Engineering

Aurangabad, Maharashtra

India

ABSTRACT

This paper presents the development of a mathematical model for tractive effort and acceleration of a small electric motor vehicle/car which is propelled by a permanent magnet direct current (PMDC) motor. The proposed vehicle acceleration model is obtained from torque-speed characteristics of the (PMDC) motor. The model is simple and it has only two vehicle parameters K_a, K_v. The vehicle parameters used in simulation are predetermined considering floor slopes. The acceleration model is simulated in MATLAB for various floor slopes and simulation performance results are presented for the vehicle that is moving on floors like flat, upslope, down slope, etc. The vehicle parameters K_a and k_v are determined with consideration of various forces that are acting on the vehicle when it is moving on different slopes. These parameters can be used in mobile robot or automated guided vehicle (AGV) navigation and also for prediction of the vehicle path.

Key Words: Modelling, Torque-speed characteristics, Simulation.

1. INTRODUCTION

The electric vehicles including fuel-cell and hybrid vehicles have been developed very rapidly as a solution to energy and environmental problems. The selection of traction motors for the electric vehicle propulsion systems is a very important step that requires special attention. In fact, the automotive industry is still seeking for the most appropriate electric propulsion system. The propulsion system must have good efficiency, reliability and low cost. There are various types of electric motors; each motor has unique torque – speed characteristics. The tractive effort developed by the motor at given load can be determined from torque – speed characteristics of the motor. The performance of the electric vehicle mostly depends on the tractive effort developed by the motor at given inputs. The mathematical modeling of electric vehicle generally consists of two sub models i.e., tractive effort and vehicle acceleration. In this paper these two sub models are proposed for selected electric motor and electric vehicle with different floor slopes. The effort has been made to give simplified model for vehicle acceleration with only two vehicle parameters K_a and K_v. The parameters K_a and K_v are associated with torque-speed characteristics of selected PMDC motor and various forces that are acting on the vehicle at different floor slopes. The torque-speed characteristics graph of selected PMDC motor is first obtained with the help of set up shown in figure 1.3.

When the vehicle moves on a surface, various forces are acting on it. The forces may be in favour or opposite to the vehicle acceleration. The forces acting against the acceleration are rolling (friction between the tyres and surface), inertia and aerodynamic drag. The grade resistance force acts in favour of the acceleration when vehicle is moving on down slope and it acts opposite to the acceleration when vehicle is moving on up slope. In this paper small eclectic vehicle is used hence aerodynamic drag is not taken into account in vehicle acceleration modeling. Secondly, the vehicle speed is to be maintained low and it is assumed that the vehicle should operate on the floor of fixed surface conditions; hence, rolling resistance force is assumed to be constant.

2. RELATED WORK

R. Akcelikand et al., have presented a comparative study of different acceleration models on the data which has been obtained from real time traffic conditions. In their study, they found polynomial model was the best for prediction acceleration distance and fuel consumption [1]. Karen L. Butler et al., have been discussed a simulation and modeling package developed at Texas A&M University, V-Elph 2.01. V-Elph facilitates in-depth studies of electric vehicle (EV) and hybrid EV (HEV) configurations or energy management strategies. It also discusses the methodology for designing vehicle drive trains using the V-Elph package [2]. Muhammad IzharIshak el at., have analyzed the performance of four-wheel drive and independent steering on an over-steer in-wheel small eclectic vehicle by using numerical simulation. Two cornering conditions were simulated i.e. steady state cornering at below critical velocity and steady-state cornering over critical velocity [3]. H. Nasiri el at., developed a hybrid electric vehicle model based on United States Department of Energy Reports and used as a benchmark for comparison. Two different power dividers in different series-parallel topologies for hybrid electric vehicles have been compared [4]. M. L. Dou el at., have developed a control-oriented drivability model for an electric vehicle. They have used least square method to identify model parameters based on the data obtained from areal eclectic vehicle [5]. Different methods in vehicle mass and road grade estimation are discussed in [6], while real time road grade estimation using onboard sensor with GPS sensor is given in [7]. Muhammad Nasiruddin Mahyuddin el at., have presented observer-based parameter estimation scheme with sliding mode term has been developed to estimate the road gradient and the vehicle weight using only the vehicle's velocity and the driving torque [8]. Jose C. Pascoa el at., proposed an alternative approach to the standard on-road coast down test used in automotive industry and in ground vehicle research [9].

3. MODELLING

The electric motor is the key component of the electric vehicle. Generally, a Permanent Magnet Direct Current (PMDC) motor is used to drive all small electric vehicle. This type of motor is very widely used in applications such as portable tools, toys, electrically operated windows in cars, and small domestic appliances such as hair dryers, etc. M.S. Widyan el at., presented the dynamical model and analysis of DC shunt, series and permanent-magnet (PM) motors fed by photovoltaic (PV) energy systems at different illuminations [10]. The characterization of small DC brushed and brushless motors can be found in [11]. The classical DC electric motor is shown in Figure 1.1. The Permanent magnet DC brushed motors (PMDC motors) consist of permanent magnets, located in the stator, and windings, located in the rotor. The ends of the winding coils are connected to commutator segments that make slipping contact with the stationary brushes. Brushes are connected to DC voltage supply across motor terminals. Change of direction of rotation can be achieved by reversal of voltage polarity. The current flow through the coils creates magnetic poles in the rotor that interact with permanent magnet poles. In order to keep the torque generation in same direction, the current flow must be reversed when the rotor north pole passes the stator south pole. For this the slipping contacts are segmented. This segmented slip ring is called Commutator. The commutator segments are made from copper. The brushes are made from precious metal or carbon (graphite brush).

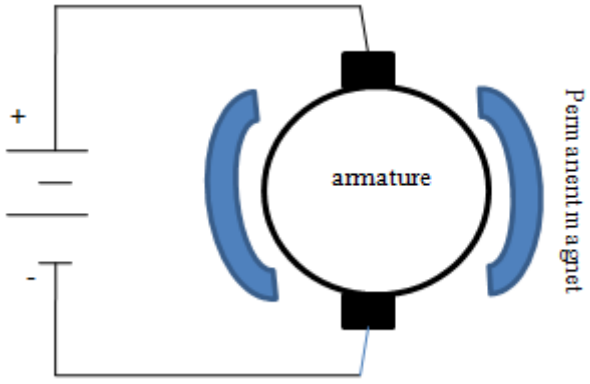

Figure 1.1: Basic construction of PMDC motor

3.1 ModellingTractive Effort

The electric motor used has one coil, and the current passing through the wire near the magnet causes a force to be generated in the coil. If a wire in an electric motor has a length *l* meters, carries a current *I* amperes, and is in a magnetic field of strength *B* Wb.m−2, then the force on the wire is:

$$F = BIL \quad (1)$$

If the radius of the coil is *r*, and the armature consists of *n* turns, then the motor torque *T* is given by the equation

DOI: 10.31695/IJASRE.2023.9.3.2

$$T = 2nrBIL \quad (2)$$

The total flux passing through the coil, the term 2Blr can be can be replaced by ϕ, this gives:

$$T = n\phi I \quad (3)$$

Equation (3), gives the peak torque, when the coil is fully in the flux, which is perfectly radial. In practice, this will not always be so. The constant K_m connects the average torque with the current and the magnetic flux. The value of $K_m$depends on the number of turns in each coil, but also on the number of pole pairs, and other aspects of motor design

$$T = K_m \phi I \quad (4)$$

Equation (4), shows that the motor torque is directly proportional to the armature current (I). This armature current is depending on supply voltage (E_s) and armature resistance (R_a). The armature current in terms of supply voltage and back emf (Eb) is given by;

$$I = \frac{V}{R_a} = \frac{E_s - E_b}{R_a} = \frac{E_s}{R_a} - \frac{K_m \phi}{R_a}\omega \quad (5)$$

Put it in (4)

$$T = \frac{K_m \varphi E_s}{R_a} - \frac{(K_m \varphi)^2}{R_a}\omega \quad (6)$$

This important equation shows that the torque from this type of motor has a maximum value at zero speed, when stalled, and it then falls steadily with increasing speed. In this analysis, we have ignored the losses in the form of torque needed to overcome friction in bearings, and at the commutator, and windage losses. This torque is generally assumed to be constant, which means the general form of (6) still holds true, and gives the characteristic graph in figure 1. 2.

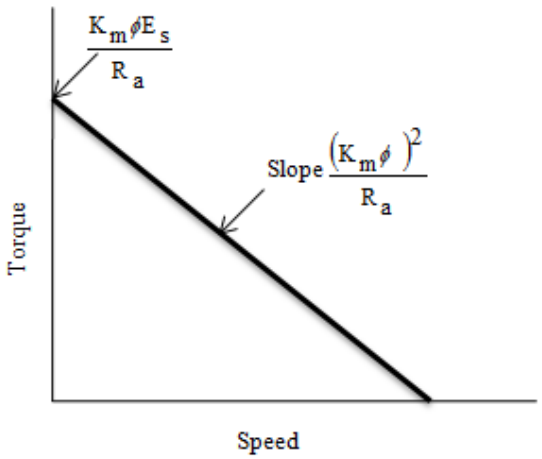

Figure 1.2: Torque –Speed graph for brushed PMDC motor

The set up shown in figure1.3 has been developed for determining the torque-speed characteristics of the motor that is used in the test vehicle. The (PMDC) motor is used in the test vehicle to apply tractive effort on the wheel to overcome vehicle resistance forces and to accelerate the vehicle. The procedure for development of equation for applied torque (tractive effort) on the vehicle wheel from torque-speed characteristics of PMDC motor is explained in section 3.1. The set up was fabricated and used to determine the torque-speed characteristics of the PMDC motor. The motor used in the test vehicle is small; hence this fabricated experimental set up is giving good results for all applied voltages and motor speeds and the setup is sufficient to determine maximum torque that motor can develop and maximum speed at no torque. For speed measurement contactless tachometer as shown in figure 1.3 (c) was used. In simulation model, the main inputs are; the maximum torque developed by the motor and maximum linear speed of the vehicle on application of that torque. Therefore, by knowing the maximum torque, the maximum angular speed of the motor, gear ratio and vehicle wheel radius, the linear speed of the vehicle on the ground or floor can be determined and used for simulation.

DOI: 10.31695/IJASRE.2023.9.3.2

The relation between motor torque (T_{motor}=T_{shaft}), angular speed ω, maximum torque (T_{max})and some constant K can be written as given by (7).This is basic equation of motor which gives torque developed by the motor at applied voltage with angular speed (ω). The constant K is the slope of torque – speed characteristics of the motor

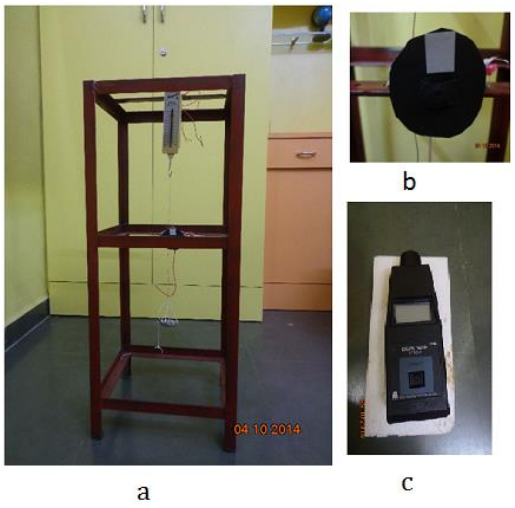

Figure 1.3: a] Motor Torque – speed characteristics set up consisting of testing structure, spring balance, load pan, motor fixing arrangement at middle of the frame; [b] Speed measurement arrangement, black circular marker with silver reflective tape enable to sense to the contactless digital tachometer and c] Contactless digital tachometer

This is basic important equation which gives the input for formulation of simulation model for electric vehicle

$$T_m = T_{\max} - K\omega \tag{7}$$

Equation (7) can be modified as;

$$T_w = T_{\max} - \frac{KG}{r}v \tag{8}$$

Equation (8) can be simplified as ;

$$T_w = T_{\max} - K_m v \tag{9}$$

Now (8) gives the tractive effort (Nm) developed by the motor which is applied on the wheels of the eclectic vehicle to accelerate it. The tractive force can be obtained from (9) by dividing tractive effort to wheel radius (r). The relation between tractive force and vehicle linear speed (V) assuming ideal conditions is presented in figure 1..4.The E_{s1} and E_{s2} indicates the supply voltage.

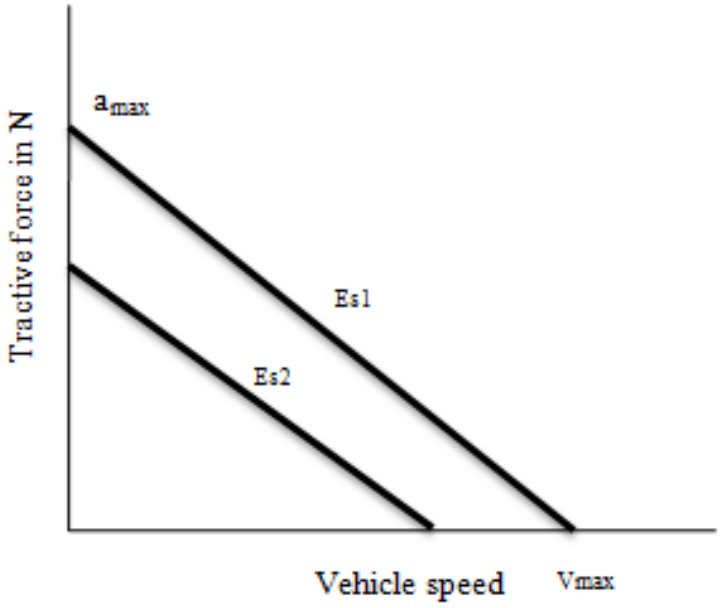

Figure 1.4: Tractive force Vs vehicle speed graph for applied voltage

DOI: 10.31695/IJASRE.2023.9.3.2

3.2 Modelling Motor Vehicle Acceleration

A problem with vehicle kinematics models is that by empirically developing mathematical expressions that describe the acceleration patterns of the vehicle, the actual components that affect the motion of the vehicle; the tractive force provided by the prime mover (PMDC motor) and the resistance forces opposing the vehicle's motion are not modeled explicitly. Therefore, these models are difficult to calibrate and do not generally provide a good fit to field data for each of the acceleration, speed, distance, and time domains. They also do not account for different vehicle types, roadway grades, and other factors that affect the vehicle acceleration patterns [12, 13]. To better account for an accelerating vehicle's actual physics of motion, a number of acceleration models have been developed based on vehicle dynamics. These models characterize the acceleration of a vehicle based on the power output from the vehicle's prime mover and power losses resulting from internal mechanical friction losses and external resistance forces, such as air resistance, rolling resistance and grade resistance forces.
In this paper, the torque- speed characteristics of the PMDC motor is used as a base for the development of acceleration model of electric vehicle. The primary equation proposed for vehicle acceleration is given as;

$$a_v = a_{\max} - \frac{a_{\max}}{v_{\max}} v \tag{10}$$

Where

a_{max}: Maximum acceleration produced by the vehicle
v_{max} : Maximum speed attained by the vehicle
a_v: Vehicle acceleration at applied force F_t
v : Speed of the vehicle at a_v

Put
$K_a = a_{max}$;
$K_{v} = a_{max}/v_{max}$;
Equation (10)can be written as;

$$a_v = K_a - K_v V \tag{11}$$

Equation (11) can be written as;

$$\frac{dV}{dt} = K_a - K_v V \tag{12}$$

After simplification (12), we can write as;

$$\frac{dV}{K_a - K_v V} = dt \tag{13}$$

Integrating (13) and putting initial conditions, velocity of the vehicle at any time 't' can be calculated by using (14).

$$V = \frac{K_a}{K_v}\left(1 - e^{-tK_v}\right) + V_0 e^{-tK_v} \tag{14}$$

Integrating (14) and putting initial conditions, distance covered by the vehicle at any given time, t can be calculated using (15).

$$S = \frac{K_a}{K_v} t - \frac{K_a}{K_v^2}\left(1 - e^{-tK_v}\right) + \frac{V_0}{K_v}\left(1 - e^{-tK_v}\right) \tag{15}$$

4. ACCELERATION MODEL SIMULATION

The acceleration model developed in section 3.2 is used for simulation. Equation (11) is integrated to obtain motor vehicle velocity and distance covered for given simulation time. The vehicle parameters K_a and K_v are determined by considering floor slopes and using data given in Table 1. The parameters calculated for given floor slope are only useful that particular slope. If the floor slope is changed the vehicle parameters must be changed and need to recalculate. The motor vehicle acceleration model is simulated on three different floor or road slopes i.e., flat slope, up slope and down slope. The motor vehicle parameters estimated

DOI: 10.31695/IJASRE.2023.9.3.2

beforehand is given in table 1. The simulation results are presented in following sections 4.1, 4.2and 4.3.The numerical solutions of (11), (14) and (15) are used for simulation in MATLAB.

Table 1 : Estimated vehicle parameters

Tractive force (F_t)	2.8 N
Rolling resistance force for flat floor	1.6 N
Grade resistance force for 3-degree floor slope	0.5 N
Vehicle mass (m)	1.02 Kg
Gear ratio(G)	9.21
Wheel radius (r)	0.024 m
Acceleration due to gravity (g)	9.81 m/s2
Vehicle maximum velocity on flat floor (V_{max})	1.2 m/s
Vehicle maximum acceleration on flat floor (a_{max})	1.18
Vehicle parameter for flat floor (K_{af})	1.18
Vehicle parameter for flat floor (K_{vf})	0.98

4.1 Motor Vehicle on Flat Slope

When the vehicle is moving on flat floor or road the forces acting against the vehicle acceleration are rolling resistance force (friction between floor and tyre) and vehicle inertia. The rolling resistance force acting on the vehicle when it is on flat slope is already determined and given in Table 1. The vehicle parameters have been set considering all forces that are acting on the vehicle. For flat floor, the values of vehicle parameters used in simulation are $K_{af} = 1.18$, $K_{vf} = 0.98$. The vehicle acceleration model is simulated in MATLAB. The simulation time was 5 seconds and two vehicle range i.e., acceleration and cruising range are covered. The distance covered, velocity gained and acceleration of the vehicle are presented in figure 1.5. The vehicle reached at peak velocity after 4 seconds of acceleration where vehicle inertia force becomes zero.

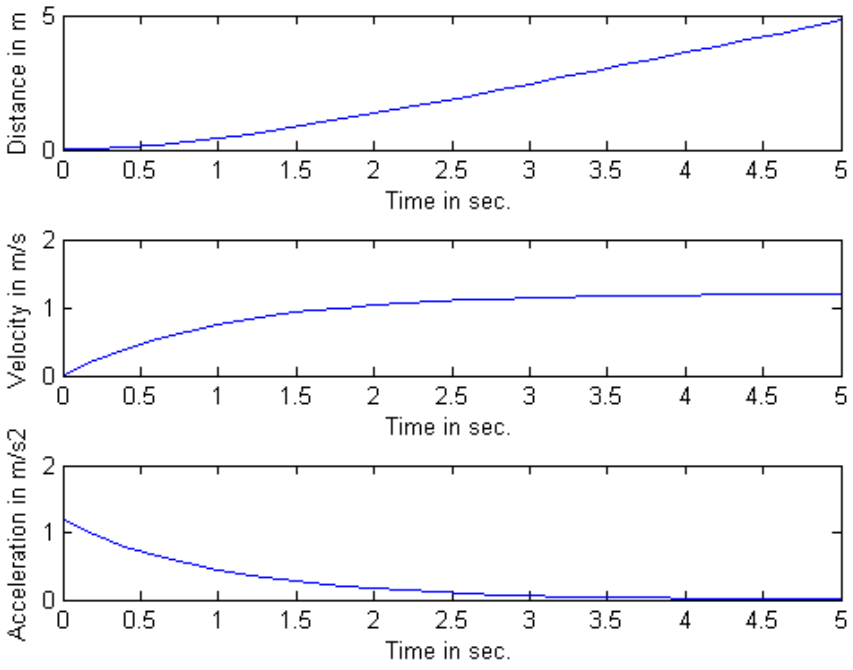

Figure 1.5: Display of simulation results of vehicle moving on flat slope

4.2. Motor Vehicle on up Slope

When the vehicle is moving on floor of up slope then the forces acting against the vehicle acceleration are rolling resistance, inertia and grade. Considering these forces, the vehicle parameters set for simulation are K_{au}=0.68, K_{vu}=1.36. These parameters are put in (11), (14), and (15) and results obtained are presented in figure 1.6, for vehicle distance covered, velocity and

DOI: 10.31695/IJASRE.2023.9.3.2

acceleration. In this case, the vehicle reached at peak velocity after 3 seconds of acceleration where vehicle inertia force becomes zero.

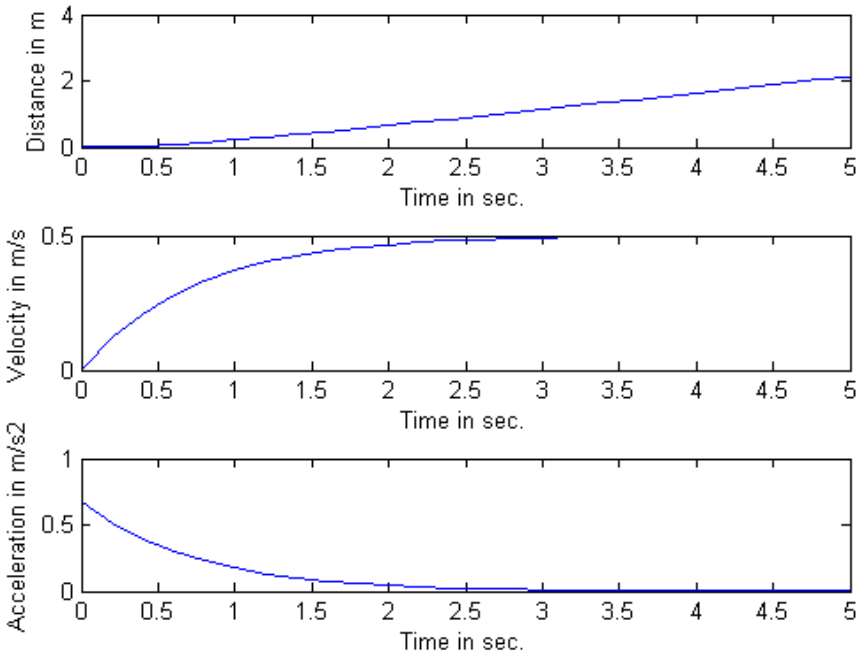

Figure 1.6: Display of simulation results of vehicle moving on upslope

4.3. Motor Vehicle on down Slope

When the vehicle is moving on floor of down slope then the forces acting against the vehicle acceleration are rolling resistance, inertia and in favour of acceleration is grade. Considering these forces, the vehicle parameters set for simulation are K_{ad}=1.67, K_{vd}=1.11. These parameters are put in (11), (14), and (15)and results obtained are presented in figure 1.7, for vehicle distance covered, velocity and acceleration. The vehicle reached at peak velocity after 5 seconds of acceleration where vehicle inertia force becomes zero.

DOI: 10.31695/IJASRE.2023.9.3.2

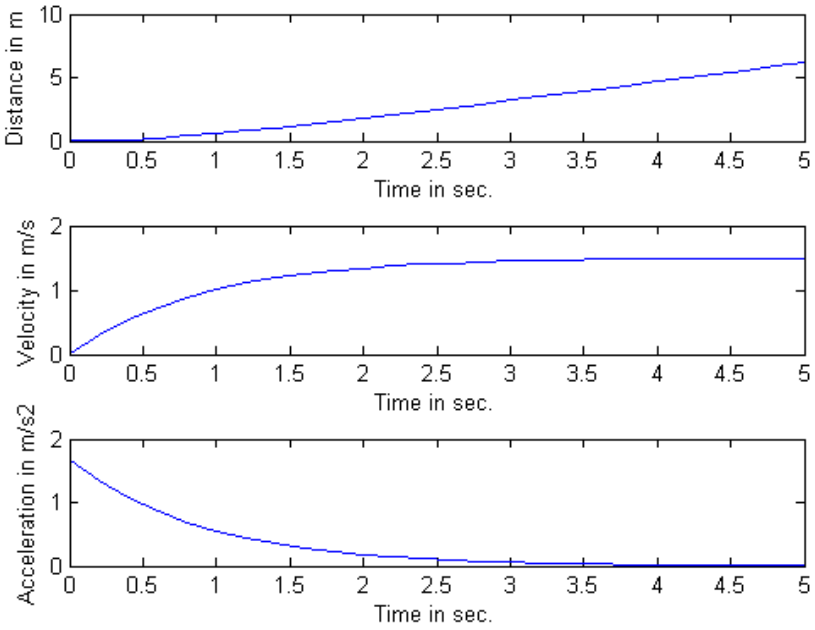

Figure 1.7: Display of simulation results of vehicle moving on downslope

4.4. Motor Vehicle Inertia Forces

The vehicle inertia force is obtained for three different floor slopes i.e., flat, up slope and down slope using vehicle parameters K_{af}, K_{vf}, K_{au}, $K_{vu,}K_{ad}$ and $K_{vd.}$ respectively. The inertia force with time for all these floor slopes are calculated and results are presented in figure 1.8.It is clear from the figure 1.8 that the inertia force is maximum at the start of the vehicle and it becomes zero when vehicle reaches its maximum speed. It is true for all floor slope conditions.

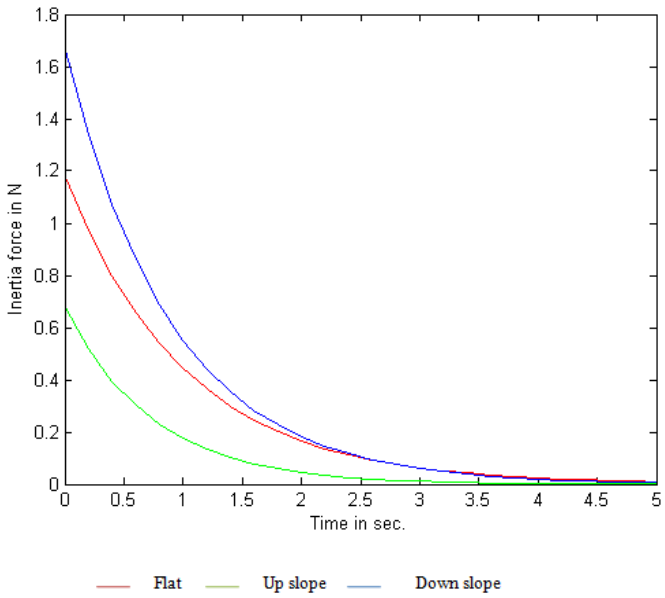

Figure 1.8: Display of inertia forces for different floor slopes

4.4. Results Comparison

The motor vehicle acceleration model presented in this paper is simulated in MATLAB for simulation time of 5 seconds each floor slope. The simulation covers two vehicle ranges i.e., acceleration and cruising. The distance covered by the vehicle during these ranges are shown in table 2. From table, it is clear that when the vehicle is on up slope it covers less distance during acceleration as compared to when it is on down slope. The total distance covered is less in it is moving on up slope for period of 5 seconds.

DOI: 10.31695/IJASRE.2023.9.3.2

Table 2: Distance covered by the vehicle on different floor slop*es*

Floor slope	Distance during acceleration in m	Distance during cruising in m	Total distance
Flat slope	3.6	1.2	4.8
Up slope	1.14	0.99	2.13
Down slope	5.3	0.87	6.17

5. CONCLUSION AND DISCUSSIONS

This paper proposes the mathematical model for tractive effort from torque-speed characteristics of PMDC electric motor and vehicle acceleration. Initially, mathematical equation for vehicle acceleration was obtained and then it solved analytically for vehicle velocity and distance with respective to the time. In vehicle acceleration equation, only two parameters K_a and K_v are used. The test vehicle used for finding various forces and parameters K_a and K_v is a small electric car. The values of these parameters for floors like flat, up slope and down slope are given in section 4.1, 4.2 and 4.3. The simulation results are validated for the vehicle when it is moving on flat floor using overhead camera sensor. However, the low field of view of camera limits the working space; the results are not getting validated for up and down slope floors.

The floor slope changes the values of parameters of K_a and K_v, because of changes in forces that are acting on the vehicle. In this paper, the values of different forces of given test vehicle and floor slope are determined beforehand and then these values are used to set the values K_a and K_v.The simulation results obtained for different floor slopes are the indication of good proposed graphs for distance, velocity and acceleration for given set conditions. There is scope for further study of these models to find the values of the K_a and K_v using vehicle position data which further can be used for vehicle path prediction and control.

REFERENCES

[1] R. Akcelikand & D. C. Biggs (1987),"Acceleration profile models for vehicles in road traffic, "Transportation Science, 21 (1), pp 36-54, 1987.

[2] Karen L. Butler, MehrdadEhsani & PreyasKamath, "A MATLAB-Based Modeling and Simulation Package for Electric and Hybrid Electric Vehicle Design", IEEE transactions on vehicular technology, Vol. 48, No. 6, pp.1770-1778,1999.

[3] Muhammad IzharIshak, Hirohikoginoand Yoshio Yamamoto, "Numerical Simulation Analysis of an Over steer In-Wheel Small Electric Vehicle Integrated with Four-Wheel Drive and Independent Steering," International Journal of Vehicular Technology Volume 2016, Article ID 7235471, 12 pages, http://dx.doi.org/10.1155/2016/7235471.

[4] H. Nasiri, A. Radan, A. Ghayebloo, "Dynamic Modeling and Simulation of Trans motor Based Series-Parallel HEV Compared to Toyota Prius 2004 Planetary Gear," J. Basic. Appl. Sci. Res., 2(12)12757-12764, 2012

[5] M. L. Dou,G Wu, Ch. Shi&X.G. lu, "Modeling and identification of longitudinal responses of an electric vehicle for drivability improvement," IJOE,Vol.9,Issue 4,http://dx.doi/10.3991/ijoe.v9i4.2821,2013.

[6] Narayanan Kidambi and R. L. Harne, Yuji Fujii Gregory M. Pietron& K. W. Wang, "Methods in Vehicle Mass and Road Grade Estimation," SAE Int. J. Passeng. Cars - Mech. Syst. 7(3), doi:10.4271/2014-01-0111,2014.

[7] Kichun Jo, Junsoo Kim, & MyounghoSunwoo, "Real-Time Road-Slope Estimation Based on Integration of Onboard Sensors With GPS Using an IMMPDA Filter," IEEE transactions on intelligent transportation system, Vol. 4 ,No4, pp.1718-1732,2013.

[8] Muhammad Nasiruddin Mahyuddin, Jing Na, Guido Herrmann XuemeiRen, & Phil Barber, "Adaptive Observer-Based Parameter Estimation With Application to Road Gradient and Vehicle Mass Estimation", IEEE transactions on industrial electronics, Vol. 61, No. 6, pp. 2851-2863, 2014

[9] Jose C. Pascoa, Francisco P. Brojo, Fernando C. Santos and Paulo O. Fael, "An innovative experimental on-road testing method and its demonstration on a prototype vehicle", Journal of Mechanical Science and Technology 26 (6) pp. 1663-1670, doi: 10.1007/s12206-012-0413, 2012

DOI: 10.31695/IJASRE.2023.9.3.2

[10] M.S. Widyan, A.I. Al Tarabsheh, I.Y. Etier,& R.E. Hanitsch, "Dynamic and steady –state characteristics of DC machines fed by photovoltaic systems", International Journal of Modeling and Simulation, Vol. 30, No.3pp.353-360,2010.

[11] Aaron M. Harrington and Christopher Kroninger, "Characterization of small DC brushed and brushless motors", U.S. Army Research Laboratory, 2013.

[12] James Larminie & John Lowry, "Electric Vehicle Technology Explained", John Wiley & Sons Ltd, 2003.

[13] Thomas D. Gillespie, "Fundamentals of vehicle dynamics, Society of Automotive Engineers", Inc, 400 commonwealth drive, Warrendale, PA 15096-000.

DOI: 10.31695/IJASRE.2023.9.3.2

Influence of Operational Variables in Bicycle Driven Bamboo Slicing Phenomena by Methodology of Response Surface Approach

Siddharth K. Undirwade

Professor & Dean IQAC, P. E. S. College of Engineering, Aurangabad-431002, M. S., India, Email: siddharthundirwade@gmail.com

Received 4 March, 2022; Revised 5 April 2022; Accepted 5 April 2022

Available online 6 April, 2022 at www.atlas-tjes.org, doi: 10.22545/2022/00174

Since global energy consumption rises, there seems to be a pressing need to create innovative technologies for saving energy and power production, especially those with lower ecological effects. There is indeed a current must to discover an alternate for renewable sources of energy to be used at any time from any location as well as being accessible to the entire public. Human energy is indeed a kind of alternative energy which has been employed to varying degrees throughout history. In this regard, this research consists of the design and construction of a pedal-driven bamboo slivering (sliver making) machine powered by a human-powered flywheel motor (HPFM). This article evaluates the overall impacts of several process factors upon the outputs of the human-powered bamboo slivering (sliver cutting) phenomenon, such as torque -resistive, sliver numbers and processing time. The 108 sets of experiments were carried out based on which experimental based models were formulated by using designed experiments and the influence of several independent (input)factors on response (output factors) variables were investigated in cutting the slivers of bamboo using an approach of response surface methodology.

Keywords: Bamboo sliver, HPFM, response surface methodology, energy, dependant variable, independent variable.

1 Introduction

The power of human and its energy was disregarded during periods of increasing utilization of fossil fuels. However, because of extremely high costs of fossil fuels and the severe pollution of environment caused by them, human power has resurfaced as a sustainable source of energy. There are serious power shortfall issues as a result of increased industrialization, as well as due to constraints on non-availability of electricity in the interior and further power generation challenges. In this sense, the energy sources are human-powered systems, which are classified as non-conventional sources of energy. Bamboo compares favorably to other materials of building such as timber, concrete and steel in terms of energy needs during

construction, simplicity of usage and safety, stiffness per unit area of material and strength. Bamboo's adaptability is partly owing to its anatomical structure, which adds to its mechanical qualities. Bamboo is the best to use everywhere due to its simplicity in production [1]. Aside from numerous of conventional methods and kinds where bamboo is largely employed for residential construction of buildings and houses, a number of commercially made items and components are used in construction of building [2]. Slivers of Bamboo are continually used for bamboo mats weaving, which have a broad range of uses such as wall paneling, handicrafts, furniture, wall papers, and so on, demonstrating the vast usage of slivers of bamboo in the industries and business manufacturing [3]. There is a significant influence of human activities on workings of Earth system such as growth in population, development of economy, and rising demands of energy. This enhances the need of dependable and reliable supply of energy that is robust to internal and external challenges which can conform unforeseen shocks in future. It is vital to emphasize that energy transformation should viewed as a means for dealing with grand energy challenges rather than global challenge [4]. In the current scenario, there is immediate requirement to identify alternative forms of power generation. The technologies of renewable or alternative energy are already acknowledged to have the potential to considerably cover the power demand resulting in reduction of emissions. To contribute to the sustainable development and prevent global catastrophe, it requires a speedy and worldwide shift to technology of renewable or alternative energy sources [5]. According to the reports and study, the renewable or alternative sources of energy may increase its proportion of total primary supply of energy from fifteen percent (in 2015) to sixty-three percent (in 2050). This probable growth of renewables along with increased energy efficiency may generate ninety-four percent of the reduction in emissions. While actual numbers may differ, the current scenario assessments agree that energy efficiency and alternative energy are more important to achieve the climate goals [6].

Alternative or renewable energies having lower environmental impacts can be considered to be only the possible solution for sustainability challenge which is been fought since long back. The global adoption of renewable energy remains restricted despite of growing knowledge of its numerous benefits. For the long term period, the traditional methods of power generation with exhaustible fuels like gas, oil and coal is usually seen as unreliable due to growing knowledge of environmental impacts [7]. Papadis, E. and Tsatsaronis, G. [8] in their paper examine the historical evolution of worldwide decarbonization facts and evaluated that technology pertaining to every sector. They assess the technological solutions whether feasible and sustainable for future trends of energy field and presented the analysis of issues in the view of economical, technical, societal and ecological challenges. The current state of affairs in the energy sector's decarbonization is far away from adequacy. Recent advances in atmospheric changes and rising emissions of carbon dioxide globally demonstrate that there is an urgent need to boost the efforts greatly for decarbonization of the energy issues [8]. Keeping view towards the severe challenges of energy crisis and its generation, many researchers have worked and are working on these issues to find out the solution. Modak J. P. and his colleagues [9 to 12] have constructed human powered machinery capable of energizing the process units requiring 3-7 HP which can be operated intermittently. The HPFM driven machines were designed and developed for wood turning [10], chaff cutter [11] and electricity generation [12] etc. which motivated the author to design and fabricate the human powered bamboo slicing machine. Sakhale, C. N. et al [13] had designed and developed the comprehensive bamboo processing machine run by an electric motor which comprises of four operations namely, (a) Bamboo cross cutting, (b) Bamboo Splitting, (c) Sliver cutting operation and (iv) Stick making. This machine is operated by means of electric motor which is again pointing towards the limitations on availability of electric power.

Therefore, with respect to a context of human powered operated systems as few of the forms of non-traditional energy, the bamboo slivering machine run by HPFM was designed, constructed and experiments were performed by identifying various process parameters (e.g. independent and dependent parameters) applying the design of experiments and experimentation theory [14]. The whole world is experiencing power and energy shortages as a result of lack of power in the interior and rural region. This is also due to various limitations on generation of additional power and energy. Thus, since this is the human operated machine and doesn't require electricity to run, this human powered machine is the best option in such energy crisis situation because the human energy is easily and globally available in ample quantity in every

corner of the world. Human energy is proven to be the form of energy which does not have any severe impacts on climate, environment and atmosphere etc. The unskilled, semiskilled operator can operate this machine easily; hence it is very useful for the people facing the problems of power shortages which add to the enhancement of bamboo technology for low profiled people from the point of view of human powered mechanization.

2 Experimental Machine Set Up

The experimental machine set up consists of three major units viz. HPFM unit is bicycle driven unit which is energy unit with a flywheel and gear pair for speed raising, Unit of transmitting mechanical power comprising of gear pair for amplification of torque and clutch, and processing unit (used to cut the bamboo sliver) which consists of sliver cutter, feeder, adjusting knobs and two pairs of spring loaded rollers etc. These three units assemble the experimental set up of human powered bamboo slivering machine as shown in figure 1. The unit of HPFM, unit of transmitting mechanical power and processing unit (bamboo sliver cutting unit) are shown in figures 2, 3 and 4 respectively.

Figure 1: *Human powered bamboo slivering machine.*

Figure 2: *HPFM Unit.*

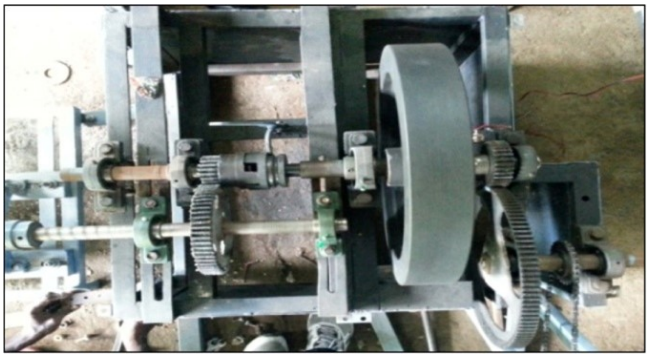

Figure 3: *Mechanical power transmission unit.*

Figure 4: *Different views of bamboo sliver cutting unit.*

2.1 Working Details of Experimental Set Up

When pedals of the bicycle driven unit are operated by operator, the energy is stored in the flywheel. Power of maximum cycling has an impact due to fatigue, rate of pedaling, composition of fiber and size of muscle. Rolling and aerodynamic friction restrict cycling speed, and any mismatch in applied vs necessary power leads to the variations in energy of the system[15]. When the flywheel stores sufficient required energy after pedaling, the flywheel energy is transmitted by engagement of clutch to the bamboo slivering unit via mechanical power transmission unit which commences the unit of bamboo sliver cutting to run. The feeder of slivering unit is fed with split bamboo which passes through the first pair of the push-in rollers and it further goes through the second pair of push-out rollers. Split bamboo strikes the cutter when it leaves push-out rollers which commence the cutting of sliver. The cutter is placed exactly in front of second pair of rollers. The sliver cutting action takes place instantly after the engagement of clutch and continues for the duration of about 5 to 20 seconds until flywheel stops rotating. The effect of increasing bicycle mass is insignificant with the most widely used gear ratios more than 1.5 [16]. The machine may be operated at various speeds by selecting the appropriate torque amplification gear ratio supplied on the slivering unit shaft. The CAD model of experimental machine set up is shown in figure 5 and that of different views of slivering unit is shown in figure 6.

The phenomena have been observed to be complicated owing to fluctuation in the dependent pi terms which fluctuates because of continual change in the angular or rotational speed of the bamboo slivering machine shaft. The variance in bamboo slivering machine shaft is decreasing rapidly. It is concerning with the resistance of operational process and inertial resistances, rely on linearly varying load torque due to fluctuations in human power or energy, bamboo material quality and non linear or varying cross sectional area of bamboo.

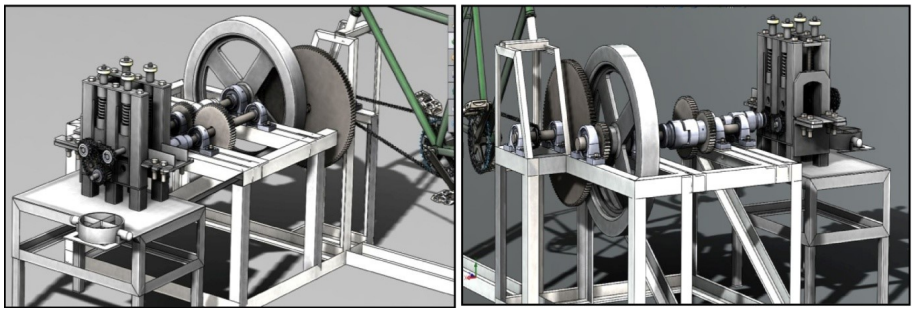

Figure 5: *CAD Model of Experimental set up (different views).*

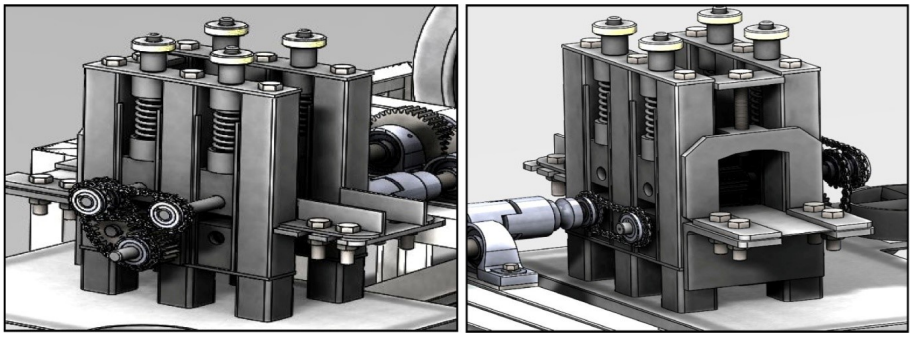

Figure 6: *CAD Model of Slivering Unit (different views).*

In the existing manual slivering machines, the manufacturers were capable of making the bamboo slivers of 1.0 to 1.5 feet long, but this HPFM driven machine can effectively manufacture the bamboo slices of 1.5 to 2.5 feet in length. The majority of the available manually operated slivering machineries are hand operated, but the present HPFM driven machine is powered by bicycle where the leg muscles are used which are marked superior to the arm muscles keeping view towards the power and energy requirements, and approaching output in the less operating time. Previously in all HPFM driven machines, most of the researchers have worked upon only the average torque of their operation. In the present research, the models are constructed for resistive torque (average) as well as resistive torque (total) in the bamboo slivering phenomena so that the influence of input factor upon the responses can be compared for both.

3 Experimental Design and Methodology

The methodology of theory of experimentation [14] was applied in this work. By applying the method of dimensional analysis using the approach of design of experiments (DoE), mathematical models for various dependent and independent process parameters were formulated after the proper determination of variables in the phenomenon of bamboo sliver cutting. Experiment design includes benefits like increasing the result attained, reducing variability, and bringing the result closer to the aim, as well as shortening the time period and lowering the cost. Several independent and dependent factors in the phenomena of cutting the slivers were identified which are shown in table 1, dimensional analysis was applied for the formation of pi-terms of all factors or parameters and independent (input) factors' pi-terms were reduced (refer table 2) to lessen the intricacy and achieve simplicity in the nature of the phenomena of cutting the slivers. Test planning to determine the experimental plan, test envelope, test sequence and test points was also performed. And after experimental design, experiment conduction and filtering or purifying experimental records, the models were formulated, optimized and reliability was also determined.

Table 1: Process parameters in sliver cutting phenomenon

Sr. No.	Parameters	Unit	Dimension	Type of Parameter
1	E_f = Stored Flywheel Energy	N-mm	ML^2T^{-2}	Independent
2	t_f = Speeding-up time of flywheel	Second	T	
3	Ω_f = Flywheel angular speed	Rad/s	T^{-1}	
4	L_b = Bamboo split length	mm	L	
5	g = Gravitational Acceleration	mm/s^2	LT^{-2}	
6	t_b = Bamboo split thickness	mm	L	
7	G = Gear Ratio	--	$M^0L^0T^0$	
8	W_b = Bamboo split width	mm	L	
9	E_c = Elastic Modulus of Cutter	N/mm^2	$ML^{-1}T^{-2}$	
10	C_H = Central (Horizontal) Distance between pairs of roller	mm	L	
11	Φ_c = Cutter's Cutting Angle	Degree	-	
12	L_{rc} = Cutter Tip to Roller Centre Distance	mm	L	
13	E_b = Elastic Modulus for Bamboo	N/mm^2	$ML^{-1}T^{-2}$	
14	C_V = Central (Vertical) Distance between pairs of rollers	mm	L	
15	n = Number of Slivers	--	$M^0L^0T^0$	Dependant
16	t_p = Processing Time	Second	T	
17	T_r = Torque (resistive)	N-mm	ML^2T^{-2}	

Table 2: Process parameters' Pi terms

Parameters	Pi terms of parameters	Equations of Pi terms	Details of Equations of Pi terms
Independent / Input parameters	π_1	$\pi_1 = \frac{E_f}{L_b^3 E_b}$	Refers to the flywheel energy
	π_2	$\pi_2 = \omega_f \sqrt{\frac{L_b}{g}}$	Refers to the flywheel angular speed
	π_3	$\pi_3 = t_f \sqrt{\frac{g}{L_b}}$	Refers to the speeding-up time of flywheel
	π_4	$\pi_4 = G$	Refers to the gear ratio
	π_5	$\pi_5 = \left(\frac{W_b t_b C_H C_V L_{rc}}{L_b^5}\right)$	Refers to the machine's geometrical parameters
	π_6	$\pi_6 = \frac{E_c}{E_b}$	Refers to the elastic modulus of materials
	π_7	$\pi_7 = \varphi_c$	Refers to cutter's cutting angle
Dependent / Output Parameters	π_{D1}	$\pi_{D1} = t_p \sqrt{\frac{g}{L_b}}$	Refers to the time of processing or operational time
	π_{D2}	$\pi_{D2} = n$	Refers to the sliver numbers
	π_{D3}	$\pi_{D3} = \frac{T_r}{L_b^3 E_b}$	Refers to the torque (resistive)

3.1 Experimental Procedure

Classical experimentation plan [14] was utilized to perform the experiment. The experiment was designed and performed to accommodate the whole test envelope along with entire test points contained in the vicinity of test envelope. All independent pi terms with the exception of one are kept fixed at their predetermined fixed level values in experimental classical plan, and the aforementioned independent pi terms within attention are changed throughout the largest feasible range as determined by the test envelope.

The experimental procedure comprises of the processing of split bamboo of different widths, of different lengths (2.5, 2.0 and 1.5 in feet) having variety of diameters (50 to 60, 40 to 50 and 30 to 40 in mm). The machining process of sliver making from bamboo was performed at four different speeds (600, 500, 400 and300 in rpm). The process was performed at different gear ratios as1/4, 1/3 and 1/2. As a result, numerous bamboo varieties are employed during experiment to assess the machine's real practicality and feasibility. With the help of specifically built electronic kit (proper instrumentation) as shown in figure 7, flywheel speeding-up time, sliver numbers, torque (resistive) and processing time etc. are estimated and noted. In this experiment, one hundred and eight total sets of readings were performed. Table 3 gives the sample observation and experiment plan. For independent parameters related to slivering unit, the experimental observations are taken and some sample observations are presented in table 4. The experimental observations for energy unit as well as for the response factors of slivering phenomena are also taken and noted which are depicted in table 5.

Figure 7: *Designed electronic instrumentation system and experimental reading generation.*

3.2 Model Formulation

During experimentation the data of various dependent and independent variables are gathered. To formulate the mathematical model, the interrelation between dependent pi terms and independent pi terms in the sliver cutting phenomena is developed. Since the formulation of the model is performed pertaining to the data produced through the experiments, it is also termed as generalized experimental model. The models formulated for the dependent variables like time of processing (t_p), sliver number (n), resistive torque-average (T_{ravg}) and resistive torque-total (T_{rtotal}) are given in equations 1, 2, 3 and 4 respectively.

$$t_P = 5.15\,X10^{-10}\sqrt{\frac{L_b}{g}}\left\{\begin{array}{c}\left(\frac{E_f}{L_b^3 E_b}\right)^{0.2889}\left(\omega_f\sqrt{\frac{L_b}{g}}\right)^{0.1564}\left(t_f\sqrt{\frac{g}{L_b}}\right)^{-0.1769} \\ (G)^{-0.3499}\left(\frac{W_b t_b C_H C_V L_{rc}}{L_b^5}\right)^{0.0371}\left(\frac{E_c}{E_b}\right)^{-3.1676}(\varphi_c)^{-30.5644}\end{array}\right\} \quad (1)$$

Table 3: Sample observations for pedal powered Slivering Operation and Plan of Experiment (where Gear Ratio = 0.33)

Sr. No.	Bamboo Diameter Range (D_b) mm	Gear Ratio (G)	Bamboo split length (L_b) ft	Bamboo split length (L_b) mm	Speed (N) rpm	Bamboo split width (W_b) mm	Bamboo split thickness (t_b) mm	Flywheel speeding-up time (ω_f) sec	Processing Time (t_p) sec	Sliver number (n)
1	40-50	0.33	1.5	457.5	300	31	4.1	31.4	60	4
2	40-50	0.33	1.5	457.5	400	31.5	4.5	41.87	55	4
3	40-50	0.33	1.5	457.5	500	31.2	4.7	52.33	70	5
4	40-50	0.33	1.5	457.5	600	31.4	4.22	62.8	80	6
5	40-50	0.33	2	610	300	35	9.1	31.4	65	4
6	40-50	0.33	2	610	400	35.1	9.6	41.87	70	5
7	40-50	0.33	2	610	500	35.5	9	52.33	85	6
8	40-50	0.33	2	610	600	35.3	9.4	62.8	95	6
9	40-50	0.33	2.5	762.5	300	25.4	15.1	31.4	45	3
10	40-50	0.33	2.5	762.5	400	24.8	15.7	41.87	60	4

Table 4: Sample Observation table showing independent factors of bamboo sliver cutting unit

	Processing unit related independent factors or input parameters														
Sr. No.	D_b (mm)	W_b (mm)	t_b (mm)	L_b (ft)	L_b (mm)	N (rpm)	ω_f (rad./s)	G	E_b (N/mm²)	E_c (N/mm²)	C_H (mm)	C_V (mm)	L_{rc} (mm)	φ_c (deg)	φ_c (rad.)
1	40-50	31	4.1	1.5	457.5	300	31.4	0.33	20000	206000	115	65	45	15	0.261667
2	40-50	31.5	4.5	1.5	457.5	400	41.86667	0.33	20000	206000	115	65	45	15	0.261667
3	40-50	31.2	4.7	1.5	457.5	500	52.33333	0.33	20000	206000	115	65	45	15	0.261667
4	40-50	31.4	4.22	1.5	457.5	600	62.8	0.33	20000	206000	115	65	45	15	0.261667
5	40-50	35	9.1	2	610	300	31.4	0.33	20000	206000	115	65	45	15	0.261667
6	40-50	35.1	9.6	2	610	400	41.86667	0.33	20000	206000	115	65	45	15	0.261667
7	40-50	35.5	9	2	610	500	52.33333	0.33	20000	206000	115	65	45	15	0.261667
8	40-50	35.3	9.4	2	610	600	62.8	0.33	20000	206000	115	65	45	15	0.261667
9	40-50	25.4	15.1	2.5	762.5	300	31.4	0.33	20000	206000	115	65	45	15	0.261667
10	40-50	24.8	15.7	2.5	762.5	400	41.86667	0.33	20000	206000	115	65	45	15	0.261667
11	40-50	25.1	15.4	2.5	762.5	500	52.33333	0.33	20000	206000	115	65	45	15	0.261667
12	40-50	25	15.6	2.5	762.5	600	62.8	0.33	20000	206000	115	65	45	15	0.261667

Table 5: Observation (sample) table for dependent factors and energy unit

Sr. No.	Energy unit related independent factors					Dependent or Output Factors	
	I_f (kg.m^2)	g (mm/s^2)	E_f (N-m)	t_f (sec)	t_p (sec)	Res. Torque- Avg. T_r (N-mm)	n
1	3.44	9810	4710.698	50	70	21692.86	3
2	3.44	9810	6783.405	35	75	23760	3
3	3.44	9810	1695.851	30	35	20728.57	3
4	3.44	9810	3014.847	35	40	23387.5	3
5	3.44	9810	4710.698	45	55	23045.45	4
6	3.44	9810	6783.405	55	60	24208.33	4
7	3.44	9810	1695.851	25	45	21711.11	2
8	3.44	9810	3014.847	30	45	23336.36	3
9	3.44	9810	4710.698	30	65	23169.23	3

$$n = 174.1406\left\{\begin{array}{c}\left(\frac{E_f}{L_b^3 E_b}\right)^{0.5082}\left(\omega_f\sqrt{\frac{L_b}{g}}\right)^{-0.3148}\left(t_f\sqrt{\frac{g}{L_b}}\right)^{-0.1208}\\ (G)^{-0.5089}\left(\frac{W_b t_b C_H C_V L_{rc}}{L_b^5}\right)^{-0.1823}\left(\frac{E_c}{E_b}\right)^{1.3087}(\varphi_c)^{-1.4871}\end{array}\right\} \quad (2)$$

$$T_{ravg.} = 1.08E + 10\left(L_b^3 E_b\right)\left\{\begin{array}{c}\left(\frac{E_f}{L_b^3 E_b}\right)^{0.7824}\left(\omega_f\sqrt{\frac{L_b}{g}}\right)^{-1.0005}\left(t_f\sqrt{\frac{g}{L_b}}\right)^{-0.351}\\ (G)^{-1.4423}\left(\frac{W_b t_b C_H C_V L_{rc}}{L_b^5}\right)^{0.0889}\left(\frac{E_c}{E_b}\right)^{4.289}(\varphi_c)^{23.515}\end{array}\right\} \quad (3)$$

$$T_{rtotal} = 7.68\,X10^{10}\left(L_b^3 E_b\right)\left\{\begin{array}{c}\left(\frac{E_f}{L_b^3 E_b}\right)^{0.7188}\left(\omega_f\sqrt{\frac{L_b}{g}}\right)^{-1.2769}\left(t_f\sqrt{\frac{g}{L_b}}\right)^{0.0101}\\ (G)^{-1.3708}\left(\frac{W_b t_b C_H C_V L_{rc}}{L_b^5}\right)^{0.0265}\left(\frac{E_c}{E_b}\right)^{-7.5718}(\varphi_c)^{6.7265}\end{array}\right\} \quad (4)$$

4 Response Surface Methodology (RSM) Approach

The response surface method's benefit as a strong analytical methodology is that, as compared to the conventional strategy, it provides a sharper visual depiction of focused connection [17]. RSM is a set of statistical as well as mathematical approaches which can be used to model and analyze issues wherein an interest response is influenced by numerous factors and the goal is to maximize this response. The RSM equation is given as:

$$Y_R = f(x_1, x_2) + E \quad (5)$$

Here, E is the error having Y_R response

x_1 is Operational parameter 1

x_2 is Operational parameter 2

Let $E(Y_R)$ be the responses expected, then it is given by:

$$E(Y_R) = \eta = f(x_1, x_2) \tag{6}$$

Here response surface is the surface that is represented or notified by, $\eta = f(x_1, x_2)$

The type of connection between independent variables and the response is uncertain & unknown in the majority of RSM applications. Hence, the RSM's first step is to discover suitable and good approximate solution to the real functional relation between collection of independent variables and Y_R. In most cases, a polynomial of lower order in some area of independent or input parameters is often used. If response modeling is done well by functional linearity of input or independent parameter, the function of approximation results in the model of first order is:

$$Y_R = \beta_0 + \beta_1 x_1 + \beta_2 x_2 + \cdots\cdots\cdots + \beta_n x_n + E \tag{7}$$

If the system has a curve, the greater degree polynomials like the model of second order must be utilized such as:

$$Y_R = \beta_0 + \sum_{i=1}^{n} \beta_i x_i + \sum_{i=1}^{n} \beta_{ii} x_i^2 + \sum \sum_{i<1}^{n} \beta_{ij}\, x_i x_j + E \tag{8}$$

The fitted surface is then utilized to perform the analysis of response surface. Analyzing the fitted surface is roughly comparable to analyze the actual data when the fitted surface is a good approximation of the underlying or real function of response.

4.1 Design of the Response Surface

Design of experiment, construction of model of response surface, testing of adaptability of model, search for optimum combination strategy and other procedures are included in the design of response surface. The accompanying second model of response surface may be utilized to generate a response surface of three-dimensions and contour line of two-dimensions, which intends to rapidly determine the correct values of response for various elements [18]. A quadratic surface can be appropriately fitted with the help of the RSM approach and aids in optimizing process variables with small number of tests/experiments while also analyzing parameter interaction. RSM is a statistical strategy that employs quantifiable information from relevant experiment to develop a model of regression and optimize an output or response parameter that is impacted by numerous input or independent factors [19]. Response Surface Approach is a descriptive statistics of experiments wherein the output is assumed to be fixed by one or more controllable parameters. The basic purpose of response surface approach is to identify an optimal response by employing a succession of experiment designs. This notion drives the need to carry out tests properly by selecting the correct design and motivates the pursuit of operating circumstances with a variety of controllable elements that result in an optimal response [20].

According to the approach of dimensional analysis adopted in this work, the total seven numbers of π terms were formed affecting the responses of the phenomena. Because these π terms are dimensionless, they may be simply divided in to three classes. To create the response surface, these three classes are transformed into 3-dimensions in space. Thus,

$$X = \pi_1 \times \pi_2 \times \pi_3, Y = \pi_4 \times \pi_5 \times \pi_6 \times \pi_7, Z = \pi_{D1} \tag{9}$$

The X, Y (input) and Z (output) ranges are more flexible and variant. As a result, the scaling of aforementioned factors X, Y (input) and Z (output) is depicted below by the use of principle of scaling:

$$x = \frac{X}{\max(X)} \ , \ y = \frac{Y}{\max(Y)} \ , \quad z = \frac{Z}{\max(Z)} \tag{10}$$

5 Construction of Model by RSM

Models of RSM in conjunction with experiment design can be used as statistical and mathematical tools. This technique not only performs well in the optimizing facts, but it has also been validated for the approach of analysis and is useful for enrichment of product [21]. The numerical as well as experimental responses can be approximated by the use of response surface approach. There is requirement of two stages such as approximation function to be well defined and design & creation of the experimental plan. Therefore, it was decided to develop RSM model and compare its performance with the mathematical model developed in this investigation. The process variable values were established to evaluate their influence on the output variables in a total of 108 tests of readings in the experiment. Response surface approach was used to plan the design of experiments and carry out the studies of behavior of process variables. By the use of "MATLAB R2009a", the construction of response surface models and the selection of acceptable models were carried out. For the output parameters, total resistive torque, sliver number, process time and average resistive torque, regression equations of best fitting for the chosen model were produced [22]. For finding out the influence of various process variables on the characteristics of output responses, the equations of response surface are derived from the data of experiments and displayed in the figures 8 to 11. Sample calculations for processing time of RSM models are given in table 6, whereas table 7 gives the concerned calculations for number of slivers. The response surface calculations are also performed for torque-average and torque-total and are presented in tables 8 and 9 respectively.

5.1 Model Construction for Processing Time

Equation of response surface or equation of polynomial of the response surface model of fifth order is evaluated and developed for output variable, processing time and is given below:

$$\begin{aligned} t_P\sqrt{\frac{g}{L_b}} = {} & 0.6522 + 0.1308x - 0.232y - 0.2394x^2 + 0.2493xy - 0.003853y^2 + 0.01659x^3 \\ & - 0.03742x^2y - 0.03488xy^2 + 0.547y^3 + 0.1101x^4 - 0.3119x^3y \\ & + 0.02459x^2y^2 + 0.02152xy^3 - 0.316y^4 - 0.03037x^5 + 0.0904x^4y \\ & + 0.03629x^3y^2 - 0.01943x^2y^3 - 0.006172xy^4 + 0.04596y^5 \end{aligned}$$

Goodness of fit: summed Square of residuals or SSE: 1.123,
R square (R^2): 0.5872,
R-square (adjusted): 0.4923,
RMSE- Root Mean Square Error: 0.1136

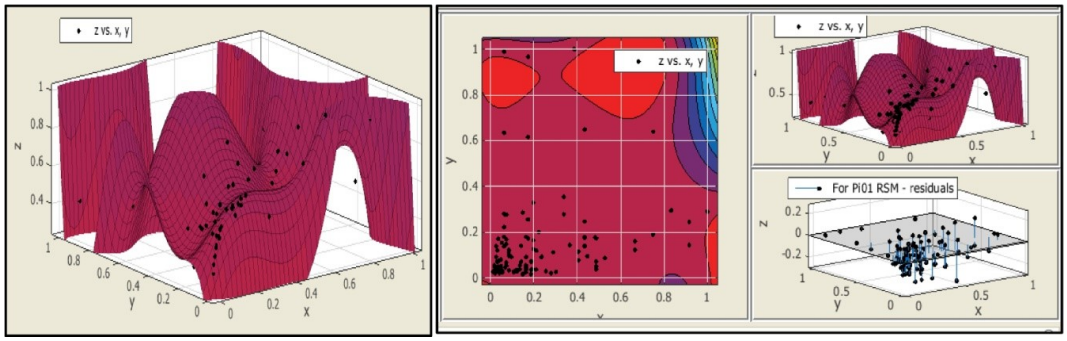

Figure 8: *RSM model and Contour, RSM and Residual plot for processing time.*

5.2 Model Construction for Number of Slivers

Equation of response surface or equation of polynomial of the response surface model of fifth order is evaluated and developed for output variable, sliver numbers and is given below:

$$n = 0.3129 + 3.279x - 0.1789y - 19.41x^2 + 7.776xy - 0.7621y^2 + 43.66x^3 + 19.83x^2y - 38.92xy^2 + 4.978y^3 - 32.36x^4 - 85.82x^3y + 39.02x^2y^2 + 44.54xy^3 - 6.561y^4 + 5.319x^5 + 56.09x^4y + 1.971x^3y^2 - 24.32x^2y^3 - 17.63xy^4 + 2.497y^5$$

Goodness of fit: summed Square of residuals or SSE: 1.188,
R square (R^2): 0.6012,
R-square (adjusted): 0.5095,
RMSE- Root Mean Square Error: 0.1169

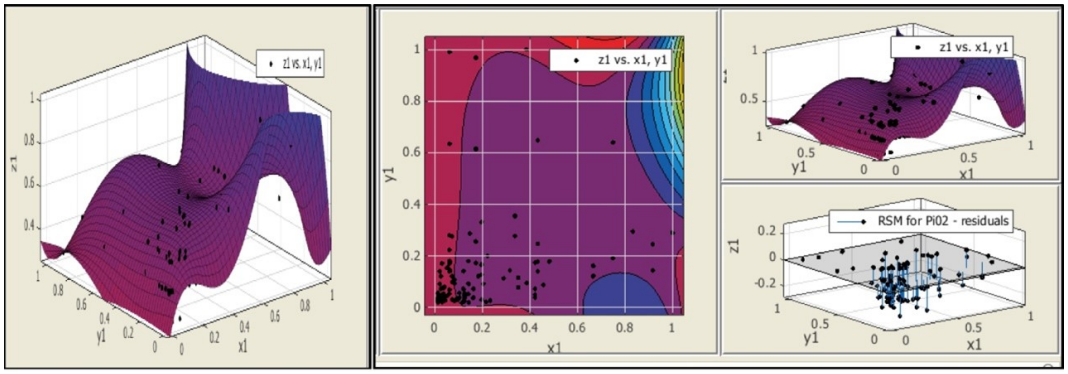

Figure 9: *RSM model and Contour, RSM and Residual plot for number of slivers.*

5.3 Model Construction for Resistive Torque (Average)

Equation of response surface or equation of polynomial of the response surface model of fifth order is evaluated and developed for resistive torque-average and is given below:

$$Avg.\frac{T_r}{L_b^3 E_b} = 0.6923 - 0.797x - 4.251y + 10.73x^2 + 5.562xy + 20.83y^2 - 35.71x^3 - 48.27x^2y + 33.36xy^2 - 55.86y^3 + 45.79x^4 + 85.2x^3y + 33.56x^2y^2 - 94.12xy^3 + 73.59y^4 - 19.5x^5 - 53.96x^4y - 20.04x^3y^2 - 5.127x^2y^3 + 56.55xy^4 - 34.83y^5$$

Goodness of fit: summed Square of residuals or SSE: 4.625,
R square (R^2): 0.2288,
R-square (adjusted): 0.05148,
RMSE- Root Mean Square Error: 0.2306

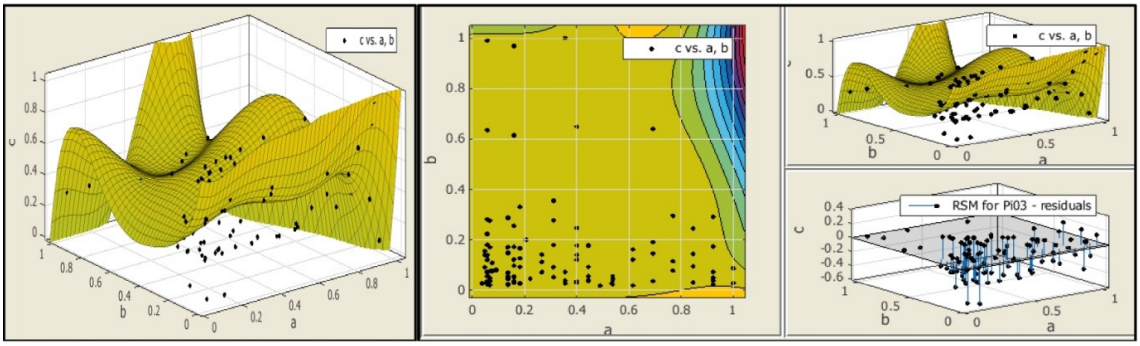

Figure 10: *RSM model and Contour, RSM and Residual plot for resistive torque (average).*

5.4 Model Construction for Resistive Torque (Total)

Equation of response surface or equation of polynomial of the response surface model of fifth order is evaluated and developed for resistive torque-total and is given below:

$$Tot.\frac{T_r}{L_b^3 E_b} = 0.4953 + 0.1362x - 2.104y - 0.1849x^2 + 6.717xy + 8.484y^2 + 1.592x^3 - 48.01x^2y + 22.54xy^2 - 22.86y^3 - 4.218x^4 + 83.75x^3y + 21.07x^2y^2 - 57.81xy^3 + 30.33y^4 + 3.145x^5 - 46.48x^4y - 28.69x^3y^2 + 11.58x^2y^3 + 29.08xy^4 - 14.14y^5$$

Goodness of fit: summed Square of residuals or SSE: 39.15,
R square (R^2): 0.1634,
R-square (adjusted): 0.1511,
RMSE- Root Mean Square Error: 0.1697

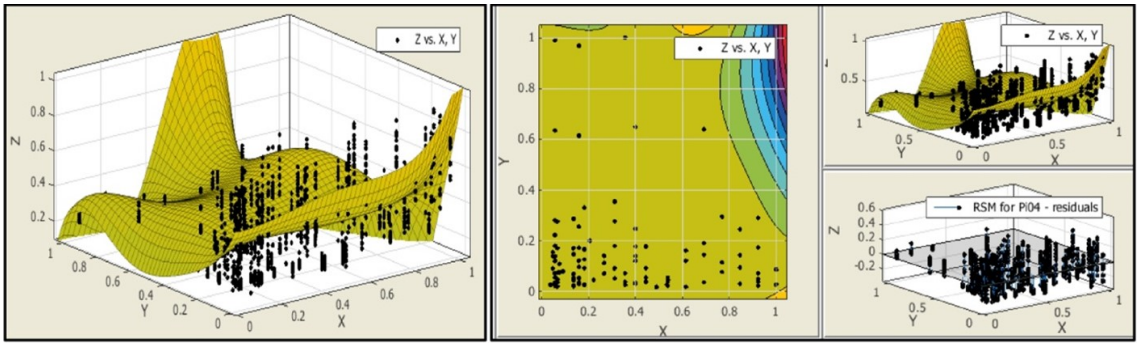

Figure 11: *RSM model and Contour, RSM and Residual plot for resistive torque (average).*

Table 6: Sample Calculation of RSM Model for processing time

Π_{D1}= tp(Model)	X=K'*Π1*Π2*Π3	Y=Π4*Π5*Π6*Π7	Π_{D1}= tp (Exp)	Π_{D1}= tp(RSM)	Xmax	Ymax	Zmax	X/Xmax =X'	Y/ymax= Y'	Z/Zmax =Z'	(Poly.Model)Z'
46.48245	1.80134E-07	3.31362E-06	40	66.92421	2.88 E-06	1.18 E-05	110	0.0625	0.280843	0.363636	0.6084
57.45825	4.26985E-07	3.3829E-06	50	68.22344	2.88 E-06	1.18 E-05	110	0.148148	0.286714	0.454545	0.62021
65.78584	9.72948E-07	3.27376E-06	50	69.84033	2.88 E-06	1.18 E-05	110	0.337577	0.277464	0.454545	0.63491
68.48212	2.88215E-06	3.4232E-06	65	64.12058	2.88 E-06	1.18 E-05	110	1	0.29013	0.590909	0.58291
41.74024	8.77505E-08	8.59642E-07	40	70.37635	2.88 E-06	1.18 E-05	110	0.030446	0.072858	0.363636	0.63978
51.47401	2.08001E-07	8.23248E-07	55	71.01566	2.88 E-06	1.18 E-05	110	0.072169	0.069774	0.5	0.6456
57.71298	5.4167E-07	8.56385E-07	60	72.05478	2.88 E-06	1.18 E-05	110	0.18794	0.072582	0.545455	0.65504
63.60235	1.17001E-06	9.23072E-07	60	72.3402	2.88 E-06	1.18 E-05	110	0.405949	0.078234	0.545455	0.65764
37.86127	5.86032E-08	4.3084E-07	45	71.1143	2.88 E-06	1.18 E-05	110	0.020333	0.036515	0.409091	0.64649
46.80633	1.38911E-07	4.41105E-07	60	71.47164	2.88 E-06	1.18 E-05	110	0.048197	0.037385	0.545455	0.64974

Table 7: Sample Calculation of RSM Model for number of slivers

Π_{D2}= n(Model)	X=Π1*Π2*Π3	Y=Π4*Π5*Π6*Π7	Π_{D2}= n(Expem)	Π_{D2}= n(RSM)	Xmax	Ymax	Zmax	X/Xmax =X'	Y/ymax =Y'	Z/Zmax =Z'	(Poly.Model)Z'
3.067968	8.34133E-07	3.31362E-06	3	3.088089	1.33 E-05	1.18 E-05	7	0.0625	0.280843	0.428571	0.44116
3.739983	1.9772E-06	3.3829E-06	4	3.978539	1.33 E-05	1.18 E-05	7	0.148148	0.286714	0.571429	0.56836
4.318878	4.50535E-06	3.27376E-06	5	4.61021	1.33 E-05	1.18 E-05	7	0.337577	0.277464	0.714286	0.6586
4.561559	1.33461E-05	3.4232E-06	5	4.844311	1.33 E-05	1.18 E-05	7	1	0.29013	0.714286	0.69204
2.460794	3.519E-07	8.59642E-07	2	2.675928	1.33 E-05	1.18 E-05	7	0.026367	0.072858	0.285714	0.38228
3.034989	8.34133E-07	8.23248E-07	3	3.256655	1.33 E-05	1.18 E-05	7	0.0625	0.069774	0.428571	0.46524
3.403551	2.17222E-06	8.56385E-07	4	3.946803	1.33 E-05	1.18 E-05	7	0.16276	0.072582	0.571429	0.56383
3.714002	4.692E-06	9.23072E-07	4	4.301708	1.33 E-05	1.18 E-05	7	0.351563	0.078234	0.571429	0.61453
1.907783	2.10202E-07	4.3084E-07	2	2.49514	1.33 E-05	1.18 E-05	7	0.01575	0.036515	0.285714	0.35645
2.324459	4.98256E-07	4.41105E-07	2	2.889732	1.33 E-05	1.18 E-05	7	0.037333	0.037385	0.285714	0.41282

Table 8: Sample Calculation of RSM Model for resistive torque-average

Π_{D3}= TrAvg(Model)	X=K'*Π1*Π2*Π3	Y=Π4*Π5*Π6*Π7	Π_{D3}= TrAvg (Expem)	Π_{D3}= TrAvg (RSM)	Xmax	Ymax	Zmax	X/Xmax =X'	Y/ymax =Y'	Z/Zmax =Z'	(Poly.Model)Z'
17182.67	1597491.83	3.31362E-06	21500	28399.7	27689858	1.18 E-05	72136.36	0.057692	0.280843	0.298047	0.39369
20248.48	3786647.302	3.3829E-06	20840	36055.76	27689858	1.18 E-05	72136.36	0.136752	0.286714	0.288897	0.49983
21692.74	8628428.096	3.27376E-06	23580	44429.01	27689858	1.18 E-05	72136.36	0.31161	0.277464	0.326881	0.6159
19978.21	25559869.29	3.4232E-06	24107.69	17368.3	27689858	1.18 E-05	72136.36	0.923077	0.29013	0.334196	0.24077
16748.77	1597491.83	8.59642E-07	24475	34518.48	27689858	1.18 E-05	72136.36	0.057692	0.072858	0.339288	0.47852
19625.27	3786647.302	8.23248E-07	20909.09	37511.39	27689858	1.18 E-05	72136.36	0.136752	0.069774	0.289855	0.52001
20191.66	9861060.681	8.56385E-07	22533.33	39424.74	27689858	1.18 E-05	72136.36	0.356125	0.072582	0.312371	0.54653
20832.13	21299891.07	9.23072E-07	25591.67	41114.09	27689858	1.18 E-05	72136.36	0.769231	0.078234	0.354768	0.56995
16054.83	1863740.469	4.3084E-07	2366.667	40160.12	27689858	1.18 E-05	72136.36	0.067308	0.036515	0.032808	0.55673
18924.21	4417755.185	4.41105E-07	2008.333	42915.66	27689858	1.18 E-05	72136.36	0.159544	0.037385	0.027841	0.59492

Table 9: Sample Calculation of RSM Model for resistive torque-total

Π_{D3}= Tr tot(Model)	X=K'*Π1*Π2*Π3	Y=Π4*Π5*Π6*Π7	Π_{D3}= Tr tot(Exp)	Π_{D3}= Tr tot(RSM)	Xmax	Ymax	Zmax	X/Xmax =X'	Y/ymax =Y'	Z/Zmax =Z'	(Poly.Model)Z'
19935.54	1597492	3.44 E-06	21700	33306.29	27689858	1.22 E-05	94600	0.057692	0.280843	0.229387	0.352075
19935.54	1597492	3.44 E-06	21900	33306.29	27689858	1.22 E-05	94600	0.057692	0.280843	0.231501	0.352075
19935.54	1597492	3.44 E-06	23500	33306.29	27689858	1.22 E-05	94600	0.057692	0.280843	0.248414	0.352075
19935.54	1597492	3.44 E-06	22700	33306.29	27689858	1.22 E-05	94600	0.057692	0.280843	0.239958	0.352075
19935.54	1597492	3.44 E-06	21000	33306.29	27689858	1.22 E-05	94600	0.057692	0.280843	0.221987	0.352075
19935.54	1597492	3.44 E-06	21400	33306.29	27689858	1.22 E-05	94600	0.057692	0.280843	0.226216	0.352075
19935.54	1597492	3.44 E-06	20100	33306.29	27689858	1.22 E-05	94600	0.057692	0.280843	0.212474	0.352075
19935.54	1597492	3.44 E-06	19700	33306.29	27689858	1.22 E-05	94600	0.057692	0.280843	0.208245	0.352075
20890.26	3786647	3.51 E-06	21700	41079.93	27689858	1.22 E-05	94600	0.136752	0.286714	0.229387	0.434249
20890.26	3786647	3.51 E-06	22200	41079.93	27689858	1.22 E-05	94600	0.136752	0.286714	0.234672	0.434249

6 Optimization of RSM Models

According to the objective function of the response variables in this human powered bamboo slicing process, RSM models' optimum values are noted from the plot of response surface model. For the maximization objective function, highest part of the plot or graph is to be selected and accordingly the values for optimization are chosen. For the minimization objective function, the lowest part of the graph is to be selected and accordingly the values for optimization are chosen. The scaled values for process time, sliver numbers, resistive torque-average and total resistive torque are shown in figures 8 to 11 respectively.

6.1 Analysis of the Models

It is of prime importance to study and note the behavior and impact of indices of the different pi terms of independent factors on all pi terms of output factors. This influence was studied and is depicted below. The indices and constants of pi terms of independent factors on output pi terms are given in Table 10.

Table 10: Indices and Constant of Response variables

Pi terms	Processing Time (tp)	Number of slivers (n)	Resistive torque-average	Resistive torque-total
K	5.15×10^{-10}	174.1406	1.08×10^{10}	7.68×10^{10}
π_1	0.2889	0.5082	0.7824	0.7188
π_2	0.1564	-0.3148	-1.0005	-1.2769
π_3	-0.1769	-0.1208	-0.351	0.0101
π_4	-0.3499	-0.5089	-1.4423	-1.3708
π_5	0.0371	-0.1823	0.0889	0.0265
π_6	-3.1676	1.3087	4.289	-7.5718
π_7	-30.5644	-1.4871	23.515	6.7265

The models for the dependent pi terms π_{D1}, π_{D2}, π_{D3} are given in equations 11, 12, 13 and 14 for process time, sliver numbers, resistive average torque and resistive total torque respectively as under:

$$\pi_{D1} = t_P\sqrt{\frac{g}{L_b}} = 5.15\times10^{-10}(\pi_1)^{0.2889}(\pi_2)^{0.1564}(\pi_3)^{-0.1769}(\pi_4)^{-0.3499}(\pi_5)^{0.0371}(\pi_6)^{-3.1676}(\pi_7)^{-30.5644} \quad (11)$$

$$\pi_{D2} = n = 174.1406\,(\pi_1)^{0.5082}(\pi_2)^{-0.3148}(\pi_3)^{-0.1208}(\pi_4)^{-0.5089}(\pi_5)^{-0.1823}(\pi_6)^{1.3087}(\pi_7)^{-1.4871} \quad (12)$$

$$\pi_{D3} = \frac{T_r}{L_b^3E_b} = 1.08\times10^{10}(\pi_1)^{0.7824}(\pi_2)^{-1.0005}(\pi_3)^{-0.351}(\pi_4)^{-1.4423}(\pi_5)^{0.0889}(\pi_6)^{4.289}(\pi_7)^{23.515} \quad (13)$$

$$\pi_{D3} = \frac{T_r}{L_b^3E_b} = 7.68\times10^{10}(\pi_1)^{0.7188}(\pi_2)^{-1.2769}(\pi_3)^{0.0101}(\pi_4)^{-1.3708}(\pi_5)^{0.0265}(\pi_6)^{-7.5718}(\pi_7)^{6.7265} \quad (14)$$

The equations 13 & 14 represent the models of resistive torque (average) and resistive torque (total) i.e.

$\pi_{D3\,Avg.}$ and $\pi_{D3Total}$ respectively. The primary conclusions of above models are described below which appear to be justified from the analysis.

(i) In case of π_{D1} and π_{D2}, the factors π_1 (refers to flywheel energy) and π_6 (refers to material elasticity) having highest indices viz.0.2889 and 1.3087 respectively, are the most influencing terms in these models. The positive values of these indices indicate that flywheel energy and material elasticity have strong impact on π_{D1} and π_{D2} respectively. Whereas for $\pi_{D3\,Avg.}$ and $\pi_{D3Total}$, the factor π_7 (refers to cutter's cutting angle) having highest indices viz.23.515 and 6.7265 respectively, are the most influencing terms in these models. The positive value of these indices indicates that there is a significant influence of cutter's cutting angle on $\pi_{D3\,Avg}$ as well as $\pi_{D3Total}$ respectively.

(ii) The factors π_5 (refers to machine's geometrical factors) having lowest indices viz. 0.0371 and 0.0889 for π_{D1} and $\pi_{D3Avg.}$ respectively is the least influencing term in these models, hence there is a need to improve machine's geometrical factors for these models of π_{D1} and $\pi_{D3\,Avg.}$ Whereas for π_{D2} and $\pi_{D3Total}$, the factors π_1 (refers to flywheel energy) and π_3 (refers to speeding-up time of flywheel) respectively are the terms which makes least influence in this model and the improvement is needed for the same.

(iii) When there are negative indices then it indicates that there is a need of improving that particular model. It shows that π_{D1} has inverse effects with π_3, π_4, π_6 and π_7, π_{D2} has inverse relationship with π_2, π_3, π_4, π_5 and π_7, $\pi_{D3\,Avg.}$ has also inverse effects with π_2, π_3 and π_4, and $\pi_{D3Total}$ has inverse impacts with π_2, π_4 and π_6.

(iv) In case of π_{D1}, the constant term is having the value less than one (i.e. 5.15×10^{-10}), and therefore it is not having effect of magnification in the calculated value from numerous term's product of this model; whereas for π_{D2}, $\pi_{D3\,Avg.}$ and $\pi_{D3Total}$, constant term had a value greater than one (i.e. 174.1406, 1.08×10^{10} and 7.68×10^{10} respectively), hence those constants have a greater effect of magnification in the calculated value from numerous term's product of their respective models.

The influence of independent or input factors in terms of sensitivity on output factors is given in table 11. This table shows the sequence of influence in increasing order from left to right.

Table11: Sequencial influence of input pi-factors upon output pi-factors

Dependent Pi-factors	**Sequence of input pi-factors as per influence**						
Processing time: Π_{D1}	π_5 (Machine's geometrical parameters)	π_2 (Flywheel angular speed)	π_3 (Speeding -up time of flywheel)	π_1 (Flywheel energy)	π_4 (Gear ratio)	π_6 (Elastic modulus of materials)	π_7 (Cutter's cutting angle)
Sliver numbers: Π_{D2}	π_3 (Speeding-up time of flywheel)	π_5 (Machine's geometrical parameters)	π_2 (Flywheel angular speed)	π_1 (Flywheel energy)	π_4 (Gear ratio)	π_6 (Elastic modulus of materials)	π_7 (Cutter's cutting angle)
Torque resistive-(average) Π_{D3} Tr-avg	π_5 (Machine's geometrical parameters)	π_3 (Speeding-up time of flywheel)	π_1 (Flywheel energy)	π_2 (Flywheel angular speed)	π_4 (Gear ratio)	π_6 (Elastic modulus of materials)	π_7 (Cutter's cutting angle)
Torque resistive-(total) Π_{D3} Tr-total	π_3 (Speeding-up time of flywheel)	π_5 (Machine geometrical parameters)	π_1 (Flywheel energy)	π_2 (Flywheel angular speed)	π_4 (Gear ratio)	π_7 (Cutter's cutting angle)	π_6 (Elastic modulus of materials)

It is notified that cutter's cutting angle is the most influencing factor in case of output factors processing time (π_{D1}), sliver numbers (π_{D2}) and resistive torque-avg ($\pi_{D3\,avg}$). But for resistive torque-total ($\pi_{D3\,total}$), elastic modulus of materials is most impacting factor. Thus overall, the cutter's cutting angle and elastic modulus of materials are having more influence on all response factors. Furthermore, machine's geometrical parameter is the least influencing factor in case of processing time (π_{D1}) and resistive torque-avg ($\pi_{D3\,avg}$) whereas speeding-up time of flywheel is having less impact on output factors like sliver numbers (π_{D2}) and resistive torque-total (π_{D3} total). Thus in general, machine's geometrical parameter and speeding-up time of flywheel are having lesser impacts on the response or output factors. The remaining input factors such as flywheel energy, flywheel angular speed and gear ratio have moderate influence over the output variables.

7 Discussion and Conclusions

(i) The properties of machining such as torque (resistive) and time of processing for human powered or pedal powered bamboo slivering process are established through theory of experiments.

(ii) Because data is acquired through real testing and actual experiments, the finding and related concluding remarks of this work accurately indicate the level of engagement of many independent factors

(iii) The analysis of the models in this research work gives the exact behaviour of the independent variables with respect to the particular response variables in terms of level of influence, level of impact, level of improvement if any etc. in case of human powered bamboo slivering machine. It also gives an idea about the magnification effects of the constants in these models.

(iv) RSM models give the scaled values for resistive torque (total), resistive torque (average), process time, and sliver numbers that are involved in the bamboo slivering machine run by pedal power.

(v) The comparative analysis of R-square value of RSM model with the formulated mathematical model gives idea of accuracy of fitness of different factors involved in the human driven bamboo sliver making phenomena. The numerical as well as experimental responses can be approximated by using the response surface approach.

(vi) The developed response surface equations and the relatively plotted graphs gives the appropriate investigation about the impact of different operational factors on numerous characteristics responses like resistive average torque, process time, resistive total torque and sliver numbers which are responsive in human driven bamboo slivering phenomena.

Funding: The author wishes to express his gratitude to the All India Council of Technical Education (AICTE), New Delhi, Govt. of India, for granting research funds via RPS (Research Promotion Scheme) to perform this research. [Grant Letter No.20/AICTE/RIFD/RPS(POLICY-III)134/2012-13, 6th March,2013].

Conflicts of Interest: The author declares no conflict of interest.

Acknowledgments: The author wishes to thank Dr. M. P. Singh and Dr. C.N. Sakhale for their useful guidance, advice and constant support during this research work.

References

[1] Janssen Jules, J. A. (1985). The Mechanical Properties of Bamboo. INBAR Bamboo Report, International Bamboo Workshop (China), 6-14, (pp. 250-256).

[2] Bamboo Brochure. Bamboo- A Material for Cost Effective and Disaster Resistant Housing. Building Materials and Technology Promotion Council (BMTPC), Ministry of Urban Development and Poverty Alleviation, Govt. of India, 1-24.

[3] Cottage Industry Manual.Bamboo MAT Weaving Techniques and Applications. Work of Mr. Yunhua, Edited & Revised by Dr. Victor Brias, UNIDO Consultant and Dr. Jinhe Fu (INBAR) under supervision of UNIDO Project Manager, Mr. Juergen Hierold, 1-29.

[4] Gribkova, D., Milshina, Y. (2022). Energy Transition as a Response to Energy Challenges in Post-Pandemic Reality. *Energies*, 15, 812, 1-26.

[5] Kumar, J., Majid, M.A. (2020). Renewable energy for sustainable development in India: current status, future prospects, challenges, employment, and investment opportunities. *Energy Sustainability and Society,* 10, 2, 1-36.

[6] Gielen, D., Boshell, F., Saygin, D., Morgan D., Bazilian, M. D., Wagner, N., &Gorini, R. (2019). The role of renewable energy in the global energy transformation. *Energy Strategy Reviews,* 24, 38–50.

[7] Seetharaman, Moorthy, K., Patwa, N., Saravanan, Gupta, Y. (2019). Breaking barriers in deployment of renewable energy. *Heliyon,* 5, 1-23. e01166.

[8] Papadis, E., Tsatsaronis, G. (2020). Challenges in the decarbonization of the energy sector. *Energy,* 205, 118025, 1-15.

[9] Modak, J. P., (2007). Human powered flywheel motor concept, design, dynamics and applications. Keynote lecture at 12th *World Congress IFToMM 2007,* Besancon, France, 17-20 June, (www.iftomm.org/iftomm/proceedings/ proceedings/A983).

[10] Modak, J. P., Bapat, A. R. (1993). Manually driven flywheel motor operates wood turning process. *Contemporary Ergonomics*, Proceedings of International Ergonomics Society Annual Convention, Edinburgh, Scotland,13-16 April, (pp 352-357).

[11] Zakiuddin, K. S., & Modak, J. P. (2010). Design and Development of the Human Energized Chaff Cutter. *New York Science Journal,* Vol.3, No. (4), 104-108.

[12] Deshpande, S. B. & Tarnekar, S. (2003). Confirming Functional Feasibility and Economic Viability of Adoption of Manually Energized Flywheel Motor for Electricity Generation. *Proceedings of International Conference on CAD/CAM Robotics Autonomous Factories*- at Indian Institute of Technology, New Delhi, Aug 11-14.

[13] Sakhale, C. N., Modak, J. P., Singh, M. P. & Bapat, P. M. (2011). Formulation of Approximate Generalised Experimental Data Based Model for Machining Properties of Bamboo. *13th World Congress in Mechanism and Machine Science*, at Guanajuato, Mexico, 19-25 June, A23-467, (pp 1-11).

[14] Hilbert Schenck J. (1968). *Theory of Engineering Experimentation.* New York, Mc Graw Hill.

[15] Martin, James C., Davidson, Christopher J., & Pardyjak, Eric R. (2007). Understanding Sprint-Cycling Performance: The Integration of Muscle Power, Resistance, and Modelling. *International Journal of Sports Physiology and Performance,* Human Kinetics, Inc., 2, 5-21.

[16] Stepniewski, Andrzej A. & Grudziński J. (2014). The influence of mass parameters and gear ratio on the speed and energy expenditure of a cyclist. *Acta of Bioengineering and Biomechancs,* Vol. 16, No. 2, DOI: 10.5277/abb140206.

[17] Lin, Hsing-Er, Hsu, Dan K. ,Hong, Michelle C. & Yongchuan Shic. (2021). Validating the response surface method in entrepreneurship management research. *Elsevier B.V.,MethodsX.*; 8: 101534, 1-7.

[18] Zheng Bin, Wang Xin, Zhang Jingdong. (2021). Structure Optimization Design for Brake Drum Based on Response Surface Methodology. *Manufacturing Technology,* Vol. 21, No. 3, 413-420.

[19] Behera, S. K., Meena, Himanshu, Chakraborty, Sudipto & Meikap, B.C. (2018). Application of response surface methodology (RSM) for optimization of leaching parameters for ash reduction from low-grade coal. *International Journal of Mining Science and Technology,* Elsevier, 28, 621–629.

[20] Joseph, Cheruiyot C., Anthony, Waititu & Anthony,Wanjoya. (2018). Response Surface Methodology in Application of Optimal Manufacturing Process of Axial-Flow Fans Adopted by Modern Industries. *American Journal of Theoretical and Applied Statistics*, 7(6), 235-241.

[21] Riswanto, FDO, Rohman A, Pramono S, Martono S. (2019). Application of response surface methodology as mathematical and statistical tools in natural product research. *Journal of Applied Pharmaceutical Science,* 9(10), 125–133.

[22] Sakhale, C.N., Waghmare, S.N., Undirwade, S.K., Sonde, V.M. & Singh, M.P. (2014). Formulation and Comparison of Experimental based Mathematical Model with Artificial Neural Network Simulation and RSM (Response Surface Methodology) Model for Optimal Performance of Sliver Cutting Operation of Bamboo. *3rd International Conference on Materials Processing and Characterisation (ICMPC 2014), Procedia Materials Science,* 6, 2211-8128 © Elsevier Ltd., (pp 877 – 891).

About the Author

Dr. Siddharth K. Undirwade is currently working as Professor Mechanical & Dean IQAC at P. E. S. College of Engineering, Aurangabad, Maharashtra, India. He is B. E. in Mechanical Engineering, M. E. in Mechanical Design and Ph. D. in Mechanical Engineering. He is having 25 years of experience in Academics, Industry and Administration in the field of Technical Education. He has also worked as the Principal of the Engineering Colleges in his tenure of working. He has published over 34 research articles in National / International Conferences / Journals so far. He is the member of Professional Societies such as Institution of Engineers (India), Indian Society for Technical Education (ISTE), Association for Machines & Mechanisms (AMM) and the Fellow of Indian Society of Mechanical Engineering etc.

MULTIDISCIPLINARY SCIENCE JOURNAL

TECHNICAL NOTE
Published Online: July 3, 2023
https://doi.org/10.31893/multiscience.2024003

Reliability approximation analysis of formulated mathematical models in pedal powered bamboo slivering operation

Siddharth K. Undirwade[a]

[a]P. E. S. College of Engineering, Aurangabad 431002, Maharashtra, India.

Abstract This paper presents the reliability approach of formulated mathematical models as well as clubbed models to examine the effects of input factors over the responses of human powered bamboo slicing phenomena. Mathematical models as well as clubbed models were developed for operational time required to cut the bamboo slivers, number or quantity of slivers to be cut and torque (resistive) required for slivering operation run by human powered flywheel motor (HPFM). Experimental data based models evolved represent various responses or output of human powered bamboo slicing phenomena. Design and fabrication of experimental set up was carried out and proper instrumentation was also decided. Design data for sliver cutting was established by the way of performing extensive experimentation. The response data was gathered which was generated by using a wide range of different independent factors by varying them. Performance characteristics were validated on the method of experimentation. The models were optimized. The reliability estimation and analysis of sensitivity was carried out for checking the effect (behavior) of various input parameters with respect to output response parameters. However, this paper entirely presents analysis of reliability evaluation of created models for various operational parameters in human powered bamboo slicing phenomena.

Keywords: human powered flywheel motor, bamboo, frequency distribution, percentage error, response factors, independent factors.

1. Preface of the Work

In present research work the design data is established for sliver cutting from bamboo energized or driven by human powered flywheel motor (HPFM). This design data was used to create the particular slivering unit (unit of sliver cutting). This design data generated through theory of experimentation can be widely and extensively useful for small industrialists, entrepreneurs and semiskilled people etc. Design data is generated and performance validation was carried out based on methods of experimentation approach suggested by Schenck Jr (1968).

Based on the design data, the experimental set-up was fabricated which comprises of basically three units viz. HPFM unit or Energy unit, Power transmission unit comprising gearing and clutch, and Process unit or Bamboo slicing unit as shown in Figures 1 and 2.

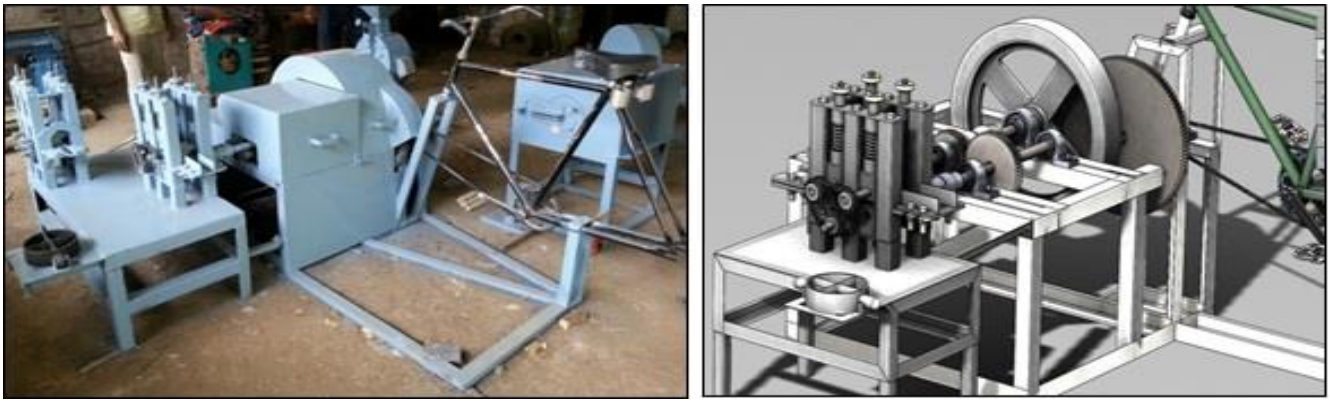

Figure 1 Fabricated Set up & its CAD model.

 Received: April 27, 2023 | Accepted: May 5, 2023

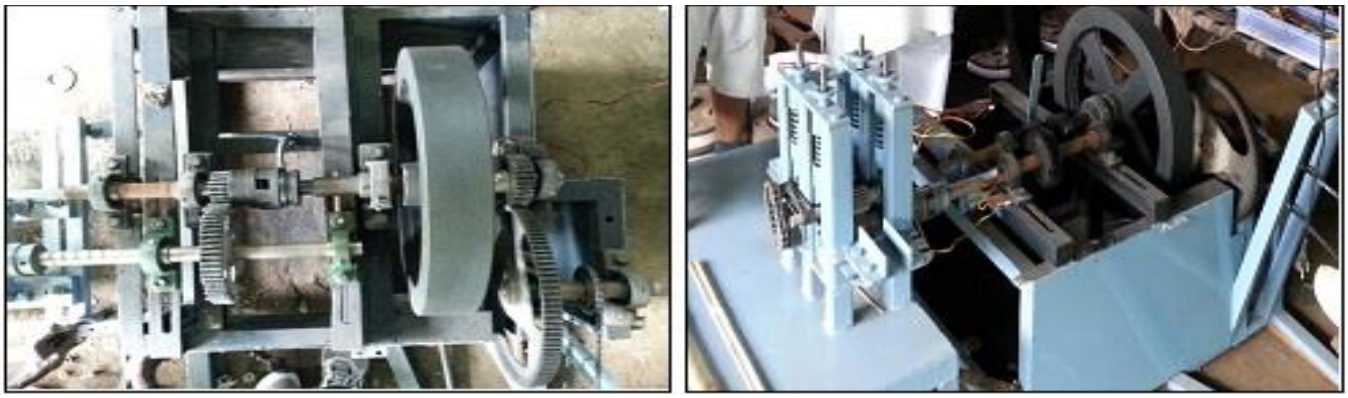

Figure 2 Energy & power transmission unit coupled with process unit.

During the experimental process, the bamboo splits of three different lengths (2.5, 2.0 and 1.5 in ft.) and varying ranges of diameter (50 to 60, 40 to 50 and 30 to 40 in mm) with various widths and thickness were processed in bamboo slivering machine at four distinct speeds (600, 500, 400 and 300 rpm) as well as at three distinct gear ratios of 1/2, 1/3, and 1/4. Hence, numerous bamboo varieties were utilized throughout experiments to analyze the machine's real and functional practicality and its feasibility. Using specially designed electronic kit, the process or operational time, torque (resistive), number or quantity of slivers, flywheel speeding up time etc. were computed (Undirwade 2022).

Methodology of experimentation was applied for design of experiments (Schenck Jr 1968). The input variables were identified like Flywheel Speed (ω_f), flywheel speeding up time (t_f), Flywheel Energy (E_f), Gravity Acceleration (g), Bamboo split thickness (t_b), Bamboo split width (W_b), Bamboo split length (L_b), Roller Center to Cutter Tip distance (L_{rc}), Vertical center distance between roller pairs (C_V), Horizontal center distance between roller pairs (C_H), Cutter Elastic Modulus (E_c), Bamboo Elastic Modulus (E_b), Cutting Angle of Cutter (Φ_c), Gear Ratio (G), and output (or response) factors such as Process or operational time (t_p), Number or quantity of slivers (n), Torque-resistive (T_r) (Undirwade et al 2017). The pi terms were formed for all input and output parameters or factors, reduction of input pi terms was carried out to reduce the complexity of the phenomenon and dimensional equations were formed for all three response variables. Then mathematical models (experimental data based models), clubbed models were formulated for checking their performance and behavior in the phenomenon (Undirwade 2018). Technique of Dimensional Analysis (DA) is used to develop theoretical models and/or predict the behavior of phenomenon, especially when the relation between dependent (response) and independent factors is not clearly known. This theoretical model developed using Dimensional Analysis (DA) can be used to cross check the empirical model developed based on experimental data. Such cross validation helps to ensure the reliability of empirical model developed (Schenck Jr 1968). The formulated mathematical models for response factors such as process or operational time, number or quantity of slivers, torque-resistive (average) and torque-resistive (total) are given in equations 1, 2, 3 & 4 respectively.

$$t_P = 5.15\,X10^{-10}\sqrt{\frac{L_b}{g}}\left\{\begin{matrix}\left(\frac{E_f}{L_b^3E_b}\right)^{0.2889}\left(\omega_f\sqrt{\frac{L_b}{g}}\right)^{0.1564}\left(t_f\sqrt{\frac{g}{L_b}}\right)^{-0.1769}\\ (G)^{-0.3499}\left(\frac{W_bt_bC_HC_VL_{rc}}{L_b^5}\right)^{0.0371}\left(\frac{E_c}{E_b}\right)^{-3.1676}(\varphi_c)^{-30.5644}\end{matrix}\right\} \quad (1)$$

$$n = 174.1406\left\{\begin{matrix}\left(\frac{E_f}{L_b^3E_b}\right)^{0.5082}\left(\omega_f\sqrt{\frac{L_b}{g}}\right)^{-0.3148}\left(t_f\sqrt{\frac{g}{L_b}}\right)^{-0.1208}\\ (G)^{-0.5089}\left(\frac{W_bt_bC_HC_VL_{rc}}{L_b^5}\right)^{-0.1823}\left(\frac{E_c}{E_b}\right)^{1.3087}(\varphi_c)^{-1.4871}\end{matrix}\right\} \quad (2)$$

$$T_{r-Avg} = 1.08E + 10(L_b^3E_b)\left\{\begin{matrix}\left(\frac{E_f}{L_b^3E_b}\right)^{0.7824}\left(\omega_f\sqrt{\frac{L_b}{g}}\right)^{-1.0005}\left(t_f\sqrt{\frac{g}{L_b}}\right)^{-0.351}\\ (G)^{-1.4423}\left(\frac{W_bt_bC_HC_VL_{rc}}{L_b^5}\right)^{0.0889}\left(\frac{E_c}{E_b}\right)^{4.289}(\varphi_c)^{23.515}\end{matrix}\right\} \quad (3)$$

$$T_{r-Total} = 7.68\ X10^{10}(L_b^3E_b)\left\{\begin{matrix}\left(\frac{E_f}{L_b^3E_b}\right)^{0.7188}\left(\omega_f\sqrt{\frac{L_b}{g}}\right)^{-1.2769}\left(t_f\sqrt{\frac{g}{L_b}}\right)^{0.0101}\\(G)^{-1.3708}\left(\frac{W_b t_b C_H C_V L_{rc}}{L_b^5}\right)^{0.0265}\left(\frac{E_c}{E_b}\right)^{-7.5718}(\varphi_c)^{6.7265}\end{matrix}\right\} \quad (4)$$

Similarly, in clubbed model all the Pi terms i.e. π_1,π_2,$\pi_3\pi_4\pi_5\pi_6$ and $\pi_7$were clubbed i.e. multiplied together and the mathematical clubbed model were subsequently constructed by the application of regression analysis. The similar analysis method was adopted as in the mathematical models formed above for developing the clubbed models for individual pi terms of all response variables. The formulated clubbed models for response factors such as process or operational time, number or quantity of slivers, resistive torque-average and resistive torque-total are given in equations 5, 6, 7 & 8 respectively.

$$t_P\sqrt{\frac{g}{L_b}} = 5654.5754\left\{\begin{matrix}\left(\frac{E_f}{L_b^3E_b}\right)\left(\omega_f\sqrt{\frac{L_b}{g}}\right)\left(t_f\sqrt{\frac{g}{L_b}}\right)\\(G)\left(\frac{W_b t_b C_H C_V L_{rc}}{L_b^5}\right)\left(\frac{E_c}{E_b}\right)(\varphi_c)\end{matrix}\right\}^{0.1149} \quad (5)$$

$$n = 56.066\left\{\begin{matrix}\left(\frac{E_f}{L_b^3E_b}\right)\left(\omega_f\sqrt{\frac{L_b}{g}}\right)\left(t_f\sqrt{\frac{g}{L_b}}\right)\\(G)\left(\frac{W_b t_b C_H C_V L_{rc}}{L_b^5}\right)\left(\frac{E_c}{E_b}\right)(\varphi_c)\end{matrix}\right\}^{0.1022} \quad (6)$$

$$\left(\frac{T_{r_{Avg}}}{L_b^3E_b}\right) = 0.00001274\left\{\begin{matrix}\left(\frac{E_f}{L_b^3E_b}\right)\left(\omega_f\sqrt{\frac{L_b}{g}}\right)\left(t_f\sqrt{\frac{g}{L_b}}\right)\\(G)\left(\frac{W_b t_b C_H C_V L_{rc}}{L_b^5}\right)\left(\frac{E_c}{E_b}\right)(\varphi_c)\end{matrix}\right\}^{0.2713} \quad (7)$$

$$\left(\frac{T_{r_{Tot}}}{L_b^3E_b}\right) = 0.000014079\left\{\begin{matrix}\left(\frac{E_f}{L_b^3E_b}\right)\left(\omega_f\sqrt{\frac{L_b}{g}}\right)\left(t_f\sqrt{\frac{g}{L_b}}\right)\\(G)\left(\frac{W_b t_b C_H C_V L_{rc}}{L_b^5}\right)\left(\frac{E_c}{E_b}\right)(\varphi_c)\end{matrix}\right\}^{0.2718} \quad (8)$$

The models were optimized and validated by means of ANN simulation (Sakhale et al 2010; Rao 1984; Rao 2002) and the values of all response (output) factors were estimated as shown in Table 1.

Table 1 Dependent/Output pi (π) terms calculated by experimental, mathematical and ANN model.

Mean/Error	t_p	n	T_r
Mean experimental	63.75	3.6667	1.10E-08
Mean ANN	57.3356	2.9537	9.43E-09
Mean math. (model)	62.6922	3.6373	1.05E-08
mean_absolute_error_performance_function (MAEPF)	11.5494	0.8717	4.12E-09
mean_squared_error_performance_function (MSEPF)	260.075	1.1088	2.42E-17
Perf	3.46E+03	23.8172	2.25E-16
% Error between model and ANN	8.544285	18.79416	10.26839
% Error between exp. and ANN	10.0618	19.44528	13.95364

The performance of all these models were checked, evaluated and also compared by performing their reliability, R^2-Coefficient of determination and sensitivity analysis. However, this paper presents only the reliability analysis of the models formulated for human powered bamboo slicing phenomenon.

2. Introduction

The term "reliability" refers to the research field that intends to provide numerical values that seeks to quantify the possibility of system failure. The term "reliability", in a very limited sense, is referred as the possibility that a system will successfully complete its goal (Sonde et al 2020). The uniqueness of this research is regarded as crucial since it is applicable to any mathematical model developed. The major goal of reliability analysis is primly to provide an efficient, precise, accurate and effective global approximation while managing the cost of computing as well as forecast accurateness or accuracy (Kernou and Bouafia 2019). One of the requirements for system design phase is to prevent or reduce the likelihood of system failure. The

system contains several components, each of which may have multiple failure scenarios. As a result, it is critical to precisely and effectively forecast system dependability during the design phase. System reliability is often treated as the likelihood that the machine or system will carry on its intended objective without problems (Hao and Xiaoping, 2020). With its development, an engineered systems become more interconnected, and function in real-time, thus reliability analysis is crucial to indicate investment and course of action. The analysis of network reliability emphasizes on a question about probability of complex machines with unreliable components and how it will behave or perform with planned specified operational circumstances (Paredes et al 2019).

Many engineering issues encounter hurdles in reliability approximations and system design because of time-varying ambiguities and performing nature. To determine the failures of machine components, Shui et al (2020) mentioned the two different classes wherein one is to determine if the product's extreme value surpasses a key threshold within the targeted lifecycle and second is to determine if the performance surpasses the highest or lowest range of the safe level for the first time throughout the planned lifecycle. Lixiong et al (2018) have stated two applications in engineering with mathematical examples to exemplify the evidence-based reliability analysis technique. It is vital to assess, regulate, and manage uncertainties in order to improve the reliability of engineering machines or structures because uncertainties in engineering analysis are unavoidable, such as environmental fluctuation, variability of material characteristics, and manufacture tolerance. The conventional random reliability technique is based mostly on probability theory, with the accompanying unpredictability of parameters expressed using a probability density function. Xiaoyue and Haiyue (2018), in their study, provided a discrete approximation approach for numerically calculating mission reliability of the systems having time redundancy in execution of mission and in reliability of higher mission. To prevent underestimating mission dependability or reliability, the influence of time redundancy should be included when evaluating the mission reliability of such systems.

Properties of material, loads applied, and structural geometrical parameters of the systems have significant uncertainties. The computation of reliability considers the consequences of these uncertainties and evaluates the structures' failure probability (Bolin and Liyang 2020). Catastrophic outcomes might emerge from industrial system failures. Engineers must cope with the growing uncertainties in order to create safe systems and avoid disastrous outcomes. The chance of failure needs to become exceedingly low for structural safety. Due to their crucial role in safety of the system, reliability approaches and their related applications have generated a significant lot of attention (Kaveh and Eslamlou 2019). Kim and Straub (2019) in their study suggested the two calculation strategies for the effective assessment of sets of reliability analyses related to various time intervals. In the general scenario, calculating a first-passage probability is necessary for the precise lifetime reliability analysis of decaying structures which might have high expenses of computation. The difficulty can be approximated by breaking it down into a sequence of time-invariant reliability issues with discrete intervals of time. Improving the quality of a multidimensional system necessitates a series of sophisticated design changes. A growing system's complexity may lead to a rise in frequency breakdown. The random and simultaneous incidence of failures or defects in a machine or system might be the primary cause of equipment performance decline. One of the strategies used to predict the lifespan of a machine and its components with many failure factors is theoretical probability distribution. A Weibull distribution which is exceptionally adaptable represents one of the most widely used statistical methods to estimate reliability (Bala et al 2018).

For time-limited tests of higher reliability and longer life systems & components, relatively minimal data of failure may be gathered. Some current approaches fail to achieve confidence interval of reliability factors and point estimation with very less data of failure. The findings are not reliable if confidence interval of reliability factors and point estimation are determined using different approaches. Zhang et al (2019) in their work developed Bayesian reliability evaluation approach for relatively lesser failure data by the use of Weibull distribution. The paper of Sabet et al (2020) highlights upon RelyFSM, a framework for state-level reliability assessment in Finite State Machines (FSM) computations. Understanding the FSM computation reliability in unstable contexts is critical for their essential functions in computing. The increasing trend of soft error rates in newest computer architecture is magnified in approximate computing where unstable hardware components are incorporated to enhance efficiency by simplifying the design of system. Radermacher and Unger (2020) proposed PGD reliability analysis wherein the structural computation solution is produced simply by assessing the PGD solution for specified set of variables without running complete finite element simulation. They presented an efficient structural reliability analysis that took advantage of the benefits of model reduction approaches to decrease the computing effort of assessing the limiting state function. This proposed method provides the path for the use of fully probabilistic methodologies in industrial applications. The environmental considerations, properties of material, external loads and dimension of various components are design parameters. They can be categorized using statistical methods. The deterministic method finds and establishes a worst-case scenario or extreme value to fulfil the design. A probabilistic method employs statistics categorization to offer the needed reliability in the design. The importance of reliability concerns extends beyond static analysis to stability analysis and dynamic analysis as well. One of the newest trends is the utilization of NN (neural networks) in hybrid reliability analysis techniques, which falls under the category of soft computational techniques (Dudzik and Beata 2019). The study by Lin and Shao (2021) established a model for the reliability evaluation as well as residual life evaluation of gas pipelines having various corrosion pits. They presented the reliability approach of Hamiltonian Monte Carlo subset simulation having benefits of high accuracy, minimum cost and lesser sampling. The reliability evaluation and estimated remained service duration of such pipeline are

crucial once it has been in use for particular length of time. By treating the input characteristics as random variables and analyzing their impact on the output response or result, the reliability technique should be employed to account for fluctuations. The random input or dependent parameters and output responses or results must have a mathematical connection in order to follow the reliability approach. Reliability connections are clear in the analytical study and are provided by traditional equations for the settlement and sustaining capacity constraints or issues (Lafifi and Rouaiguia 2021).

Wang et al (2022) studied in their work, the issues of correlation and complexity during Approximate Computing Circuit (ACC) reliability evaluation. They provide iterative Probabilistic Transfer Matrix-based ACC reliability evaluation techniques that are quite accurate and comprehensive. With the rising significance and availability of approximate computing circuit (ACC) reliability evaluation, there is high necessity of reliability assessment methods to assess their fault vulnerability. Two precise reliability assessment techniques for approximation computing circuits have been provided for computation of reliability. The iterative Probabilistic Transfer Matrix model (PTM model) is used to determine the dependability of approximation computing circuits. Many variables in a system that may be viewed as random variables and that follow a particular statistical distribution include applied loads, resistance characteristics, material attributes, and dimensional factors. For estimating failure probability, the First Order Reliability Methodology offers the most ease, especially for the relatively small or compact structure. Using a more challenging calculation method, the Second Order Reliability Methodology could offer a result that is comparatively reliable and accurate (Wang 2022). Uncertainties in constructional dimensions, interference due to change in environment, properties of material, etc. are common and unavoidable, and they are major source of instability and even system performance failure. The industry's growing need for lighter, economical and efficient systems makes it increasingly crucial demanding to analyze system reliability while taking uncertainties into account. Many reliability computation techniques and mathematical statistics based probabilistic methods have been employed to address the system's constructional uncertainties. The probability techniques analyze the dependability and system safety through the computation of the probability statistical theory and utilize the precise probability distribution function (PDF) to express the unpredictability of the factors. It is essential to examine effective system reliability analysis techniques employing non-probabilistic approaches. This analysis is helpful to acquire more satisfactory reliability analysis results for the critical structural reliability (Li and Liu 2022). The goal or objective of reliability assessment is to find out the likelihood such that a system shall survive in an unknown situation or fail in that situation. One of the most common uncertain models in the reliability evaluation field is the model of probability, in which the structural uncertainties are characterized as random parameters. The reliability techniques simulate the functional performance at MPP (i.e., most probable point) of limit-state surface which has the higher most probability density. The structural system reliability evaluation has been given a lot of thought over the past years due to the emphasis on system security, and it is now unquestionably crucial in the system design process. The likelihood of failure sensitivity values in relation to the probability distribution are accepted for the random variables (Zakaria et al 2017).

Thus, keeping view towards the significance of analysis of reliability estimation, the present paper specifically highlights upon reliability approximations of formulated models for bamboo slivering process to evaluate the behavior of various operational parameters involved in the human powered bamboo slicing phenomena. The signified importance of this research is regarded as crucial since it is applicable to any mathematical model developed. The error frequency distribution for created models was carried out using a graphical depiction and comparison of these graphs was carried out with commonly and frequently used probability density function graphs of life distributions.

3. Model Reliability Approximation

Plotting graphs of the error frequency distribution for created models is method for assessing a model's reliability. The probability density functional graphs of commonly and frequently used life distributions were compared to these graphs. Frequency distribution is most common and general case in statistical computing or analysis. Different reliability factors and characteristics are modelled using a variety of statistical distributions (Irwin and Marylees 2003). The specific distribution that is employed depends upon the type of data being examined and evaluated. By the comparison of error frequency graphical representation of different mathematical models with probability density functional graphs of commonly and frequently applied life distribution, the reliability approximation of model was executed (Ebeling 2004).

3.1. Frequency distribution of Error for mathematical model

In this experiment, there were observed and computed sets of values for the dependent factors or parameters viz. process or operational time, number or quantity of slivers and torque (resistive) of manual bamboo sliver cutting operation. The difference of observed set of value and computed set of value is an error. Frequency rates of incidence or occurrence for particular errors were evaluated for three models of response factors in bamboo sliver cutting operation as representative sample. Tables 2, 3, 4 and 5 show the frequency distribution of error for response factors' mathematical models of π_{D1}, π_{D2}, $\pi_{D3(Avg.)}$ and $\pi_{D3(Total)}$ respectively.

Table 2 Frequency distribution of error for response factor, process or operational time (mathematical model of π_{D1}).

% of Error f_i (1)	Frequency x_i (2)	$f_i x_i$ (3)	% of Error f_i (1)	Frequency x_i (2)	$f_i x_i$ (3)
0	2	0	20	1	20
1	5	5	21	4	84
2	4	8	22	1	22
3	5	15	23	1	23
4	4	16	25	1	25
5	4	20	26	2	52
6	4	24	28	1	28
7	5	35	29	1	29
8	6	48	31	3	93
9	2	18	32	1	32
10	4	40	33	2	66
11	4	44	34	1	34
12	7	84	35	1	35
13	2	26	39	1	39
14	5	70	42	1	42
15	8	120	44	1	44
16	3	48	50	1	50
17	5	85	61	1	61
18	1	18	74	1	74
19	2	38	**859**	**108**	**1615**

Error (Mean)	$\sum \frac{fixi}{xi}$	14.953704
Reliability	$\mathbf{100 - Error\ (Mean)}$	85.046296 %

Table 3 Frequency distribution of error for response factor, number or quantity of slivers (mathematical model of π_{D2}).

% of Error f_i (1)	Frequency x_i (2)	$f_i x_i$ (3)	% of Error f_i (1)	Frequency x_i (2)	$f_i x_i$ (3)
0	8	0	16	5	80
1	7	7	17	4	68
2	7	14	18	3	54
3	5	15	19	2	38
4	5	20	20	1	20
5	3	15	21	2	42
6	5	30	23	2	46
7	2	14	24	2	48
8	6	48	26	1	26
9	2	18	28	1	28
10	6	60	29	1	29
11	6	66	32	1	32
12	6	72	34	1	34
13	5	65	36	1	36
14	5	70	56	1	56
15	2	30	**519**	**108**	**1181**

Error (Mean)	$\sum \frac{fixi}{xi}$	10.9351852
Reliability	$\mathbf{100 - Error\ (Mean)}$	89.0648148 %

Table 4 Frequency distribution of error for response factor, resistive torque- average (mathematical model of $\pi_{D3(Avg.)}$).

% of Error f_i (1)	Frequency x_i (2)	$f_i x_i$ (3)	% of Error f_i (1)	Frequency x_i (2)	$f_i x_i$ (3)
0	1	0	10	8	80
1	3	3	11	6	66
2	9	18	12	7	84
3	2	6	13	1	13
4	5	20	14	1	14
5	13	65	15	2	30
6	22	132	16	2	32
7	14	98	24	1	24

8	13	104			
9	18	162	**160**	**128**	**951**

Error (Mean)	$\sum \frac{fixi}{xi}$	7.429688
Reliability	$\mathbf{100 - Error\ (Mean)}$	92.57031 %

Table 5 Frequency distribution of error for response factor, resistive torque- total (mathematical model of $\pi_{D3(Total)}$).

% of Error f_i **(1)**	**Frequency x_i** **(2)**	$f_i x_i$ **(3)**	**%Error f_i** **(1)**	**Frequency x_i** **(2)**	$f_i x_i$ **(3)**
0	65	0	46	3	138
1	71	71	47	1	47
2	54	108	48	2	96
3	61	183	49	2	98
4	62	248	50	1	50
5	70	350	51	1	51
6	58	348	52	1	52
7	58	406	53	2	106
8	68	544	54	2	108
9	53	477	55	2	110
10	45	450	57	2	114
11	40	440	58	2	116
12	51	612	60	1	60
13	53	689	61	1	61
14	47	658	62	2	124
15	46	690	63	2	126
16	35	560	64	1	64
17	36	612	65	4	260
18	34	612	66	1	66
19	33	627	67	3	201
20	30	600	68	3	204
21	22	462	69	1	69
22	23	506	70	4	280
23	33	759	71	4	284
24	11	264	72	3	216
25	20	500	73	4	292
26	11	286	74	1	74
27	9	243	75	2	150
28	8	224	76	1	76
29	9	261	77	3	231
30	11	330	78	1	78
31	16	496	79	2	158
32	7	224	80	1	80
33	3	99	81	1	81
34	5	170	83	1	83
35	8	280	84	2	168
36	4	144	85	1	85
37	2	74	86	4	344
38	2	76	87	1	87
39	4	156	89	1	89
40	3	120	91	1	91
41	3	123	95	1	95
42	4	168	98	1	98
43	3	129	99	1	99
44	3	132	100	3	300
45	2	90	**4203**	**1380**	**21461**

Error (Mean)	$\sum \frac{fixi}{xi}$	15.551449
Reliability	$\mathbf{100 - Error\ (Mean)}$	84.448551

3.2. Error frequency distribution for clubbed model

Tables 6, 7, 8 and 9 show the frequency distribution of error for response factors' clubbed models of π_{D1}, π_{D2}, $\pi_{D3(Avg.)}$ and $\pi_{D3(Total)}$ respectively.

Table 6 Frequency distribution of error for response factor, process or operational time (clubbed model of π_{D1}).

% of Error f_i (1)	Frequency x_i (2)	$f_i x_i$ (3)	% of Error f_i (1)	Frequency x_i (2)	$f_i x_i$ (3)
0	2	0	24	3	72
1	6	6	25	2	50
2	1	2	26	2	52
3	1	3	27	3	81
4	2	8	28	4	112
5	1	5	29	2	58
6	3	18	30	1	30
7	4	28	31	1	31
8	2	16	33	1	33
9	6	54	35	2	70
10	4	40	36	4	144
11	4	44	37	1	37
12	4	48	39	1	39
13	2	26	43	1	43
14	9	126	44	1	44
15	2	30	45	1	45
16	4	64	47	2	94
18	3	54	48	2	96
20	4	80	56	2	112
21	2	42	59	2	118
22	3	66			
23	1	23	**982**	**108**	**2144**

Error (Mean)	$\sum \frac{fixi}{xi}$	19.8518519
Reliability	$\mathbf{100 - Error\ (Mean)}$	80.1481481

Table 7 Frequency distribution of error for response factor, number or quantity of slivers (clubbed model of π_{D2}).

% of Error f_i (1)	Frequency x_i (2)	$f_i x_i$ (3)	% of Error f_i (1)	Frequency x_i (2)	$f_i x_i$ (3)
0	8	0	24	1	24
1	5	5	26	1	26
2	3	6	27	1	27
3	3	9	28	1	28
4	6	24	29	1	29
5	4	20	30	1	30
6	4	24	33	2	66
7	3	21	34	1	34
8	5	40	35	2	70
9	2	18	36	1	36
10	6	60	41	1	41
11	5	55	42	2	84
12	4	48	43	1	43
13	5	65	47	2	94
14	4	56	53	1	53
15	2	30	54	1	54
16	1	16	55	1	55
17	2	34	63	1	63
18	2	36	68	1	68
19	4	76	75	1	75
20	2	40	100	1	100
22	1	22			
23	2	46	**1198**	**108**	**1851**

Error (Mean)	$\sum \frac{fixi}{xi}$	17.1388889
Reliability	$\mathbf{100 - Error\ (Mean)}$	82.8611111

Table 8 Frequency distribution of error for response factor, average torque (resistive) (clubbed model of $\pi_{D3(Avg.)}$).

% of Error f_i (1)	Frequency x_i (2)	$f_i x_i$ (3)	% of Error f_i (1)	Frequency x_i (2)	$f_i x_i$ (3)
0	6	0	19	2	38
1	4	4	20	2	40
2	10	20	21	3	63
3	8	24	22	2	44
4	7	28	23	1	23
5	6	30	25	3	75
6	9	54	26	3	78
7	6	42	28	2	56
8	2	16	30	1	30
9	6	54	33	3	99
10	2	20	34	1	34
11	3	33	35	2	70
12	3	36	36	1	36
13	6	78	41	1	41
14	5	70	43	1	43
15	2	30	46	1	46
16	3	48	48	1	48
17	7	119	59	1	59
18	2	36	**760**	**128**	**1665**

Error (Mean)	$\sum \frac{fixi}{xi}$	13.00781
Reliability	$\mathbf{100 - Error\ (Mean)}$	86.99219

Table 9 Frequency distribution of error for response factor, total torque (resistive) (clubbed model of $\pi_{D3(Total)}$).

% of Error f_i (1)	Frequency x_i (2)	$f_i x_i$ (3)	% of Error f_i (1)	Frequency x_i (2)	$f_i x_i$ (3)
0	26	0	50	22	1100
1	14	14	51	18	918
2	19	38	52	21	1092
3	11	33	53	17	901
4	14	56	54	17	918
5	18	90	55	21	1155
6	18	108	56	17	952
7	13	91	57	16	912
8	17	136	58	11	638
9	13	117	59	13	767
10	15	150	60	10	600
11	11	121	61	16	976
12	21	252	62	9	558
13	21	273	63	8	504
14	13	182	64	4	256
15	11	165	65	12	780
16	22	352	66	5	330
17	16	272	67	11	737
18	15	270	68	5	340
19	17	323	69	9	621
20	9	180	70	4	280
21	12	252	71	4	284
22	15	330	72	11	792
23	20	460	73	6	438
24	8	192	74	7	518
25	22	550	75	3	225
26	19	494	76	1	76
27	14	378	77	9	693
28	18	504	78	5	390
29	19	551	79	4	316
30	19	570	80	6	480
31	11	341	81	3	243
32	19	608	83	5	415

33	15	495	84	4	336
34	18	612	85	4	340
35	17	595	86	4	344
36	21	756	87	2	174
37	21	777	89	5	445
38	16	608	90	1	90
39	11	429	91	6	546
40	16	640	92	4	368
41	16	656	93	1	93
42	18	756	94	2	188
43	10	430	95	4	380
44	18	792	96	2	192
45	7	315	97	3	291
46	21	966	98	2	196
47	10	470	99	4	396
48	16	768	100	204	20400
49	17	833	**4880**	**1380**	**64335**

Error (Mean)	$\sum \frac{fixi}{xi}$	46.61957
Reliability	$\mathbf{100 - Error\ (Mean)}$	53.38043

4. Establishing the Model's reliability

4.1. Establishing the Mathematical Model's reliability

The mathematical formula for reliability is:

$$R = 1 - MeanError$$

and computation of error (mean) is calculated by the formula:

$$MeanError = \frac{\sum f_i \times x_i}{\sum f_i}$$

Tables 2, 3, 4 and 5 show the reliability estimation or calculations in bamboo sliver cutting operation by HPFM for mathematical models of entire three response or dependent π-terms.

Here, f_i - Frequency (occurrence frequency) of occurrence, and

x_i- Percentage of error.

The total system reliability for the system in series is depicted by the equation:

Reliability of System,

$$R_s = 1 - \prod_{i=1}^{n}(R_i)$$

Computation of reliability of system in parallel is indicated by the equation:

$$R_p = 1 - \prod_{i=1}^{n}(1 - R_i)$$

Hence, for such case total system reliability in parallel is provided by:

$$R_p = 1 - \prod_{i=1}^{n}(1 - R_i) = 1 - \{(1 - R_{itp})(1 - R_{in})(1 - R_{iTr})\}$$

Where, R_p - total system reliability in parallel

R_{itp} - reliability for model of process or operational time (π_{D1}),

R_{in} - reliability for model of number or quantity of slivers (π_{D2}), and

R_{iTr} - reliability for model of torque-resistive (π_{D3})

Since during the experimental process, simultaneous observations were recorded and identified;

Thus, for the models of bamboo slivering phenomena, the total reliability is:

$= 1 - \{(1 - 0.850462)(1 - 0.890648)(1 - 0.9257031)\} = 0.9987817 = 99.8781\ \%$

(Here the value of average torque (resistive) is substituted as 0.9257031 against R_{iTr})

Therefore, Reliability of machine or system = $\mathbf{99.8781}\ \%$

If the value of total torque (resistive) is substituted as $R_{iTr} = 84.448551\ \%$,

Then, for the models of bamboo slivering phenomena, the total reliability is:

$= 1 - \{(1 - 0.850462)(1 - 0.890648)(1 - 0.844485)\} = 0.997456 = 99.7456\ \%$

Therefore, Reliability of machine or system = $\mathbf{99.7456}\ \%$

4.2. Establishing the Clubbed Model's reliability

The clubbed model's reliability for the machine is established in the same fashion like mathematical models. Tables 6, 7, 8 and 9 show the reliability estimation or calculations in bamboo sliver cutting operation by HPFM for clubbed models of entire three response or dependent π-terms.

Thus, for the models of bamboo slivering phenomena, the total reliability is:

$= 1 - \{(1 - 0.801481)(1 - 0.828611)(1 - 0.8699219)\} = 0.995574 = 99.5574\ \%$

(Here the value of average torque (resistive) is substituted as 0.8699219 against R_{iTr})

Therefore, Reliability of machine or system = $\mathbf{99.5574}\ \%$

If the value of total torque (resistive) is substituted as $R_{iTr} = 53.38043\ \%$,

Then, for the models of bamboo slivering phenomena, the total reliability is:

$= 1 - \{(1 - 0.801481)(1 - 0.828611)(1 - 0.5338043)\} = 0.984138 = 98.4138\ \%$

Therefore, Reliability of machine or system = $\mathbf{98.4138}\ \%$

5. Reliability approximation of model

5.1. Reliability approximation of mathematical model

The reliability of the developed models can be approximated similar to the reliability of the standard life distribution. On the basis of frequency distribution analysis of sample models for three approaches, graphs were plotted for frequency Vs error. Figures 3, 4, 5 and 6 depict the graph of frequency Vs error for various mathematical models of the human powered bamboo sliver cutting operation.

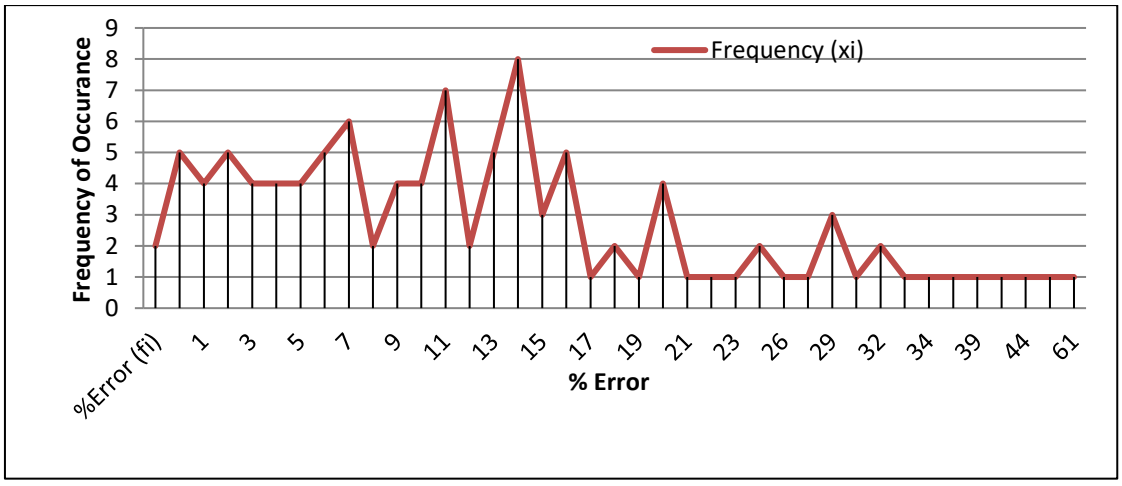

Figure 3 Error frequency graph of mathematical model for processing time, tp (π_{D1}).

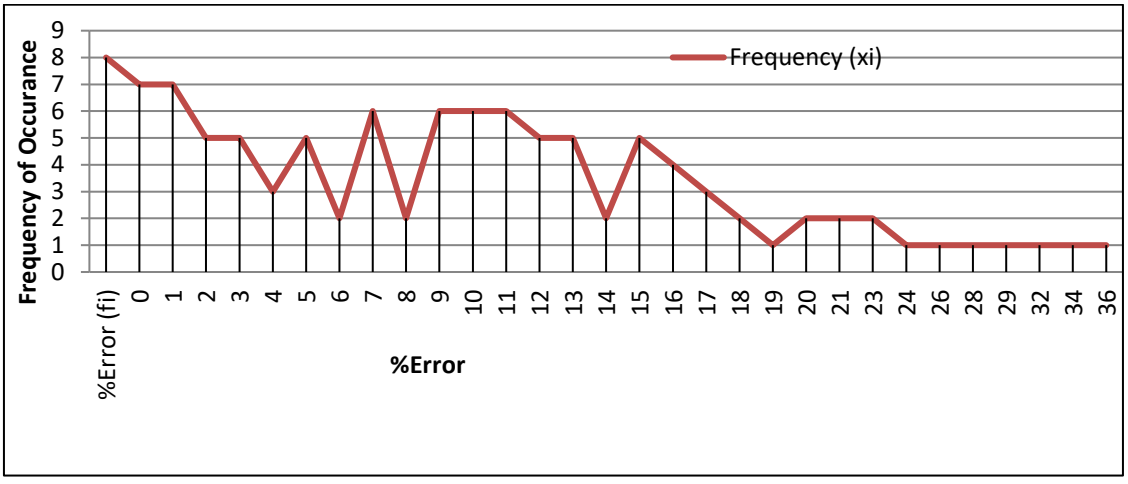

Figure 4 Error frequency graph of mathematical model for number or quantity of slivers, n (π_{D2}).

The comparison of these error frequency graphs was carried out with graphs of probability density function of standard distributions. It is noticed that different portion of the graph confirmed to some of standard distribution i.e. normal, lognormal,

exponential and Weibull. These distributions have different reliability. Thus reliabilities of these models as well as these distributions are equal.

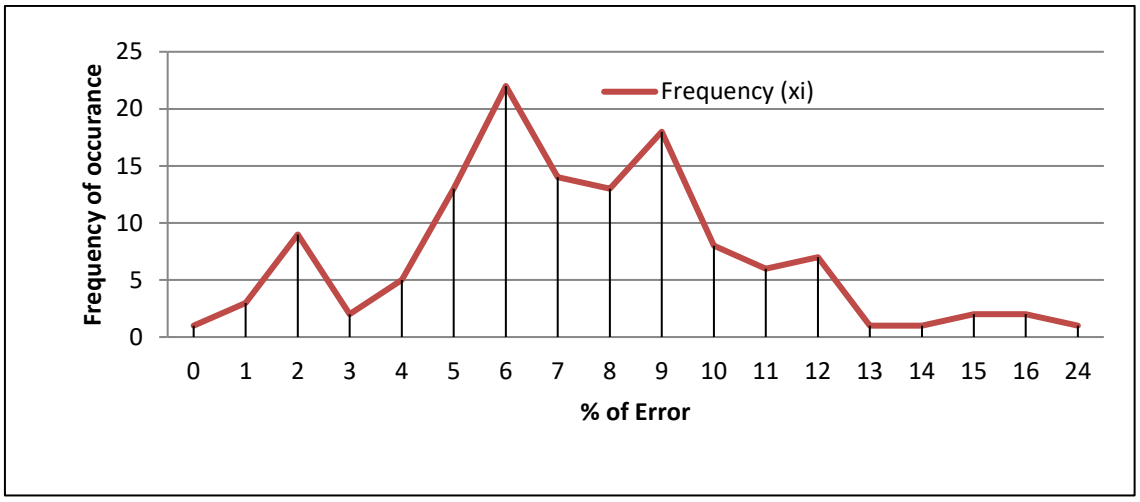

Figure 5 Error frequency graph of mathematical model for resistive torque-average, $T_{r\text{-}avg}$ ($\pi_{D3\text{-}Avg}$).

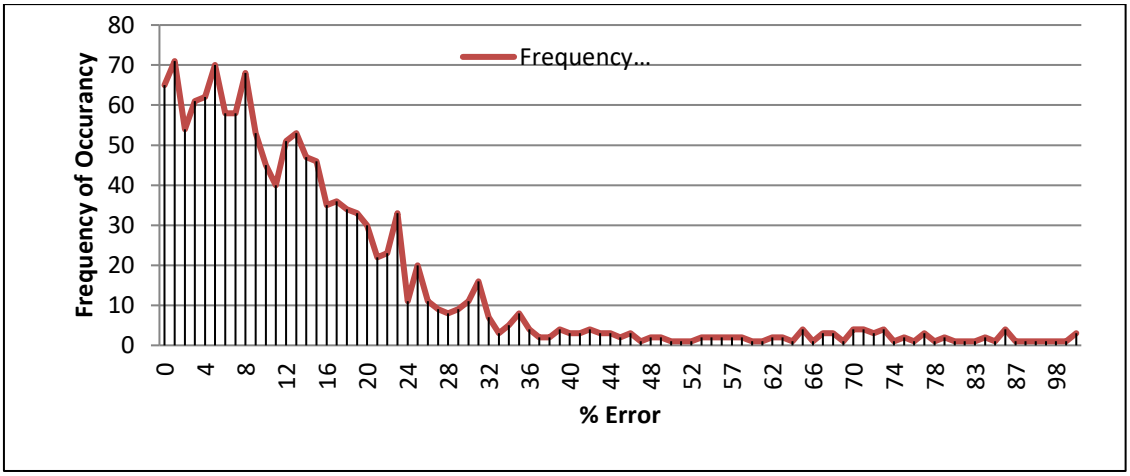

Figure 6 Error frequency graph of mathematical model for resistive torque-total, $T_{r\text{-}total}$ ($\pi_{D3\text{-}Total}$).

5.2. Reliability approximation of clubbed model

Figures 7, 8, 9 and 10 depict the graph of frequency Vs error for various clubbed models of the bamboo sliver cutting operation by HPFM.

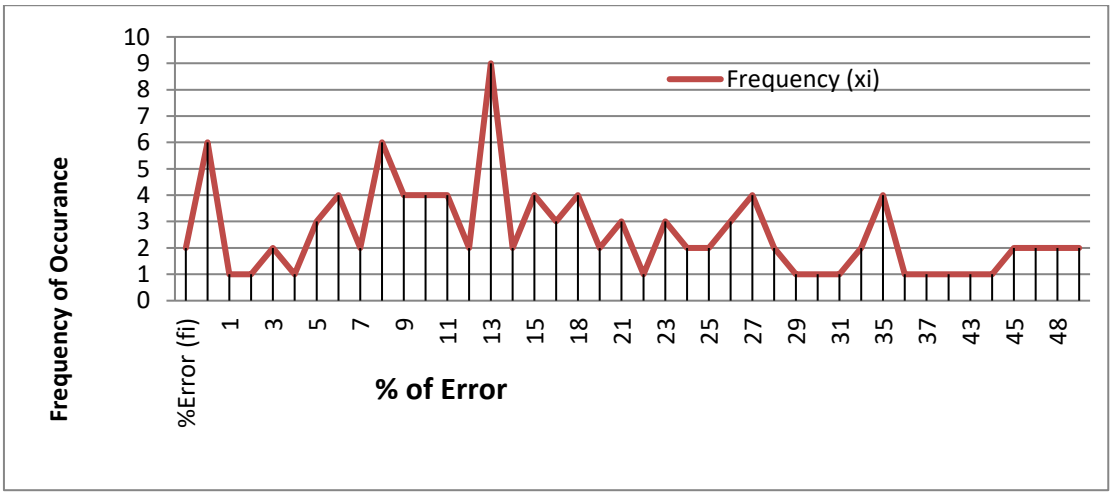

Figure 7 Error frequency graph of clubbed model for processing time, t_p (π_{D1}).

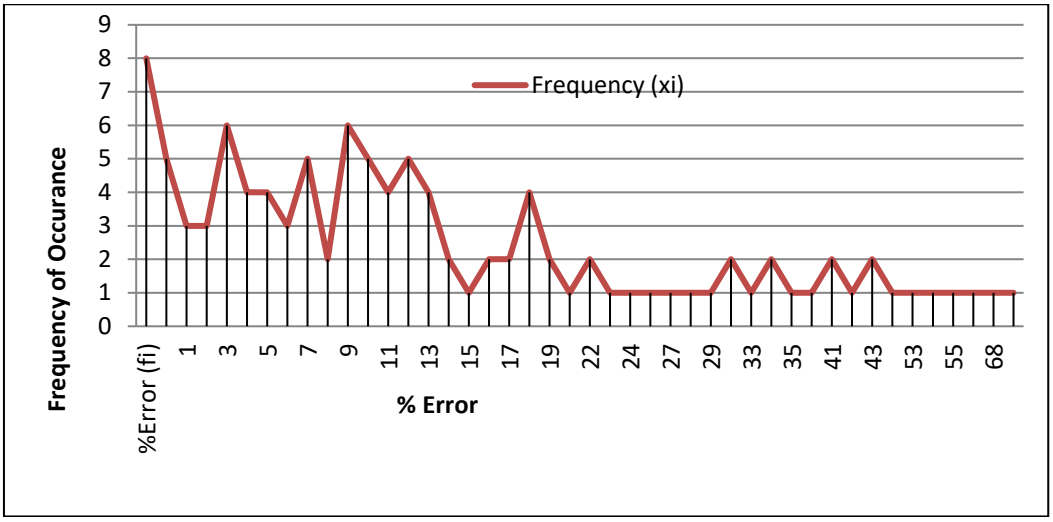

Figure 8 Error frequency graph of clubbed model for number of slivers, n (π_{D2}).

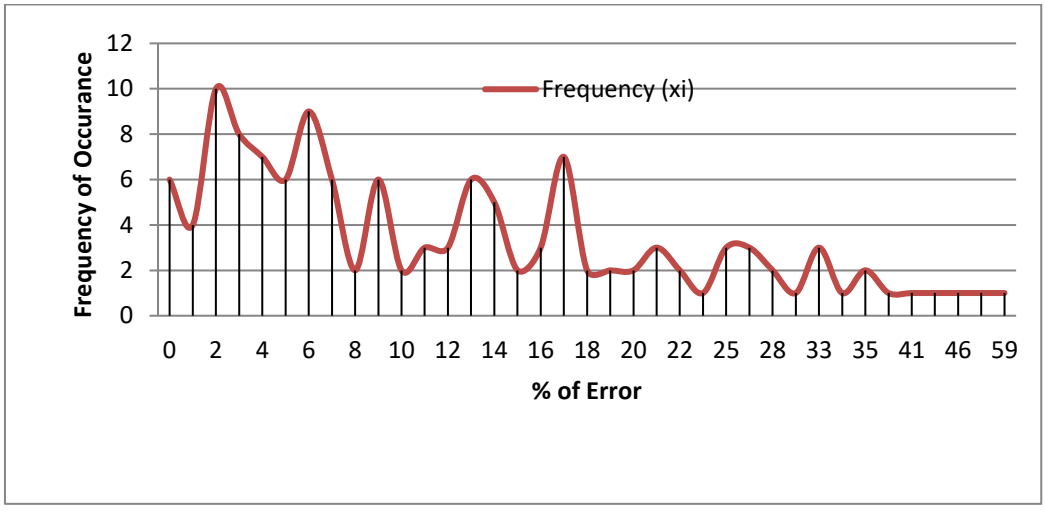

Figure 9 Error frequency graph of clubbed model for resistive torque-average, $T_{r\text{-}avg}$ ($\pi_{D3\text{-}Avg}$).

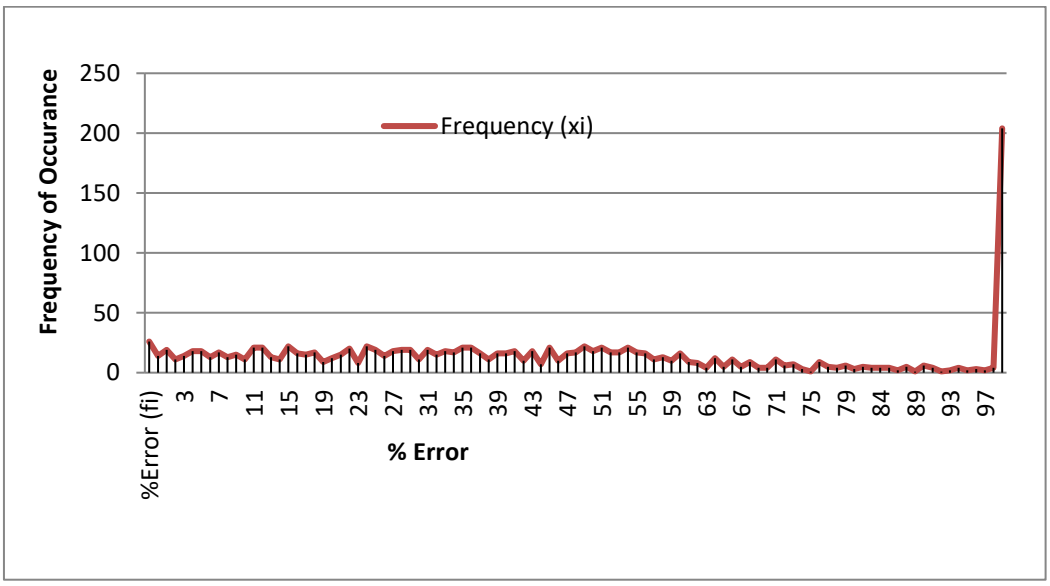

Figure 10 Error frequency graph of clubbed model for resistive torque-total, $T_{r\text{-}total}$($\pi_{D3\text{-}Total}$).

The mathematical models' reliability and clubbed models' reliability are compared and is given in following Table 10.

Table 10 Comparison of the % Reliability for mathematical models and clubbed models of π_{D1}, π_{D2}, and π_{D3}.

π term	% Reliability for mathematical models	% Reliability for clubbed models
π_{D1} (Operational Time)	85.0462	80.1481
π_{D2} (Number or quantity of slivers)	89.0648	82.8611
$\pi_{D3\text{-}Avg}$ i.e. average resistive torque	92.57031	86.99219
$\pi_{D3\text{-}Total}$ i.e. total resistive torque	84.4485	53.38043
System Reliability when $T_{r\text{-}avg}$ is taken into consideration	99.8781	99.5574
System Reliability when $T_{r\text{-}total}$ is taken into consideration	99.7456	98.4138

6. Conclusions

This paper has emphasized on the reliability evaluation approach of mathematical models and clubbed models formulated for the manually driven bamboo slicing machine. Reliability approximation is based on the standard life distribution and associated probability density functions. From the comparative analysis of graphs of error frequency with probability density function it is observed that the models' reliability and the reliability of standard distributions are equivalent. The comparison of percentage reliability of mathematical as well as clubbed models is made. From this comparative data, it is revealed that reliability concerns of mathematical models are found better than that of approach of clubbed models.

From table 10, it is noted that the reliability of mathematical model for processing time (π_{D1}) is 85.0462 %, whereas for clubbed model is 80.1481 %, the reliability of mathematical model for number of slivers (π_{D2}) is 89.0648 %, whereas for clubbed model is 82.8611 %, the reliability of mathematical model for average resistive torque ($\pi_{D3\text{-}Avg}$) is 92.57031 %, whereas for clubbed model is 86.99219 % and the reliability of mathematical model for total resistive torque ($\pi_{D3\text{-}Total}$) is 84.4485 %, whereas for clubbed model is 53.38043 %. Here, our mathematical models formulated are better reliable than clubbed models. The total machine or system reliability is found to be 99.8781 % and 99.5574 % for mathematical models and clubbed models respectively in case of resistive torque-average ($T_{r\text{-}avg}$) whereas it is found to be 99.7456 % and 98.4138 % for mathematical and clubbed models respectively in case of total resistive torque ($T_{r\text{-}total}$).

There is very little standardized error in the estimation of predicted and/ or computed values of response or dependent factors. This adds credibility to the mathematical models that have been established. It has been seen from the percentage error values that the mathematical models may be employed effectively for computing of response factors with respect to given collective set of distinct independent factors. The reliability analysis of formulated models for this manually driven bamboo slicing machine proved to be robust in construction to process any sizes and/or varieties of bamboo. The study of this analysis reveals that the economic or financial concerns, feasibility and designing data of this machine is authentic and useful for entrepreneurs, however it may vary from place to place depending on the working condition and environment since this model formulation was carried out considering Indian environmental conditions and species of bamboo. The experimental data in this study was gathered through carrying out actual genuine experiments, therefore the findings of this study accurately reflect the interaction level between different independent factors. The behavior pattern of the mathematical models and clubbed models demonstrated for graphical reliability analysis proves the authenticity of the formulated mathematical models for human powered bamboo slivering operation. The scope may be highlighted such as the obtained models of this study were formulated considering local conditions of manufacturing facilities, local available bamboo samples, workmanship of fabrication and environmental conditions. The adopted models can be applied to other working and environmental conditions and the behavior of these models can be confirmed.

Acknowledgment

The author would like to thank Dr. M. P. Singh and Dr. C. N. Sakhale for their constant guidance and support to complete this research work.

Ethical considerations

Not applicable.

Conflict of Interest

The author declares no conflicts of interest.

Funding

This research work was funded by All India Council of Technical Education (AICTE), New Delhi, Govt. of India, under RPS (Research Promotion Scheme), vide Grant Letter No.20/AICTE/RIFD/RPS(POLICY-III)134/2012-13, 6th March,2013.

References

Bala RJ, Govinda RM, Murthy CSN (2018) Reliability analysis and failure rate evaluation of load haul dump machines using Weibull distribution analysis. Mathematical Modelling of Engineering Problems 5:116-122.

Bolin L, Liyang X (2020) An Improved Structural Reliability Analysis Method Based on Local Approximation and Parallelization. Mathematics 2020:1-13. DOI: 10.3390/math8020209.

Dudzik A, Potrzeszcz-Sut B (2019) The structural reliability analysis using explicit neural state functions. MATEC Web of Conferences 262, 10002, KRYNICA 2018, 1-6, DOI: 10.1051/matecconf/201926210002

Ebeling CE (2004) An Introduction to Reliability and Maintainability Engineering. Tata McGraw Hill Publications.

Hao W, Xiaoping D (2020) System Reliability Analysis with Second-Order Saddlepoint Approximation. ASCE-ASME Journal of Risk and Uncertainty in Engineering Systems, Part B: Mechanical Engineering 6:041001-1-041001-8.

Hyun-Joong K, Straub D (2019) Efficient Computation of the Lifetime Reliability of Deteriorating Structures13th International Conference on Applications of Statistics and Probability in Civil Engineering, ICASP13 Seoul, South Korea, 1-8, May 26-30, 2019.

Irwin M, Marylees M (2003) John E Freund's Mathematical Statistics with Applications7th Edition. Pearson education.

Kaveh A, Eslamlou AD (2019) An efficient method for reliability estimation using the combination of asymptotic sampling and weighted simulation. Scientia Iranica, Transactions A: Civil Engineering 26:2108-2122.

Kernou N, Bouafia Y (2019) Development of New Approach in Reliability Analysis for Excellent Predictive Quality of the Approximation Using Adaptive Kriging. International Journal of Engineering Research in Africa 44:44-63. DOI: 10.4028/www.scientific.net/jera.44.44

Lafifi B, Rouaiguia A (2021) Investigation of reliability analysis of shallow foundation by combining Hasofer-Lind index, response surface methodology and multi-objective genetic algorithm. Int J Reliability and Safety 15:18-36.

Li K, Liu H (2022) Structural Reliability Analysis by Using Non-Probabilistic Multi-Cluster Ellipsoidal Model. Entropy 24:1-19. DOI: 10.3390/e24091209

Lin X, Shao G (2021) Application of HMC-SS Method in Pipeline Reliability Analysis and Residual Life Assessment. Mathematical Problems in Engineering, 1-10. DOI: 10.1155/2021/3756441

Lixiong C, Jie L, Xu H, Chao J, Qiming L (2018) An efficient evidence-based reliability analysis method via piecewise hyperplane approximation of limit state function. Structural and Multidisciplinary Optimization 58:201–213.

Paredes R, Duenas-Osorio L, Meel KS, Vardi MY (2019) Principled Network Reliability Approximation: A Counting-Based Approach. Reliability Engineering & System Safety 191:1-36.

Rao SS (1984) Optimization Theory & Applications (2nd Ed.) Wiley Eastern Ltd.

Rao SS (2002) Engineering Optimization (third ed.) New Age International (p) Limited publishers: New Delhi.

Radermacher AR, Unger JF (2020) Efficient structural reliability analysis by using a PGD model in an adaptive importance sampling schema. Advance Modeling and Simulation in Engineering Sciences 7:1-29. DOI: 10.1186/s40323-020-00168-z

Sabet AHN, Junqiao Q, Zhijia Z, Krishnamoorthy S (2020) Reliability Analysis for Unreliable FSM Computations. ACM Transactions on Architecture and Code Optimization 17:1-23.

Sakhale CN, Modak JP, Singh MP, Bapat PM (2010) Design of experimentation and application of methodology of engineering experimentation for investigation of processing torque, energy and time required in bamboo processing operations. Journal of Bamboo and Rattan 9:13-27.

Schenck H Jr (1968) Theories of Engineering Experimentation. Mc Graw Hill New York.

Shui Y, Yanwei Z, Li Y, Zhonglai W (2020) Time-variant reliability analysis via approximation of the first-crossing PDF. Structural and Multidisciplinary Optimization 62:2653-2667.

Sonde VM, Warnekar PN, Ashtankar PP, Ghutke VS (2020) Calculation of Reliability Approximation of Mathematical Model Formed for Manually Operated Wood Chipper. Advances in Lightweight Materials and Structures.

Undirwade SK (2022) Influence of Operational Variables in Bicycle Driven Bamboo Slicing Phenomena by Methodology of Response Surface Approach. Transdisciplinary Journal of Engineering & Science 2:23-41.

Undirwade SK, Singh MP, Sakhale CN (2017) Formulation of Mathematical Model for Processing Time Required for Bamboo Sliver Cutting Using HPFM. Materials Today: Proceedings 4:10174-10178.

Undirwade SK (2018) Development and Optimization of Experimental Data Based Models for Bamboo Sliver Cutting by Using Human Powered Flywheel Motor. International Journal of Mechanical and Production Engineering Research and Development (IJMPERD) 8:1007-1020.

Wang L (2022) Research Methods for Reliability Analysis of Engineering Structures Based on Statistical Theory. Highlights in Science, Engineering and Technology, 28, AGECT 2022:94-100.

Wang Z, Zhang G, Ye J, Jiang J, Li F, Wang Y (2022) Accurate Reliability Analysis Methods for Approximate Computing Circuits. Tsinghua Science and Technology, 27:729-740.

Xiaoyue W, Haiyue Y (2018) Approximation method for reliability of one-unit repairable system with time redundancySafety and Reliability – Safe Societies in a Changing World 2389-2392.

Zakaria EH, Bendaou O, Bakkali LE (2017) Numerical Approximation of Structural Reliability Analysis Methods. International Journal of Innovation and Applied Studies 19:276-282.

Zhang L, Guang J, Yang, Y (2019) Reliability Assessment for Very Few Failure Data and Weibull Distribution. Mathematical Problems in Engineering 1-9.